REPORT OF INVESTIGATION 67

STATE OF ILLINOIS

DEPARTMENT OF REGISTRATION AND EDUCATION

Hydraulic Jump Type Stilling Basins for Froude Number 2.5 to 4.5

by NANI G. BHOWMIK

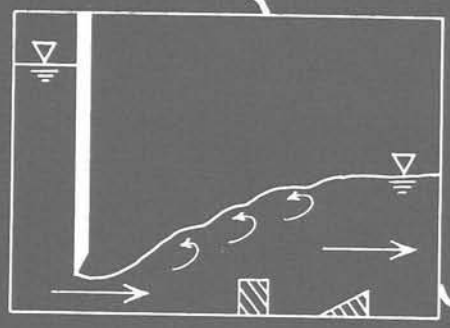

ILLINOIS STATE WATER SURVEY

URBANA

1971

REPORT OF INVESTIGATION 67

Hydraulic Jump Type Stilling Basins for Froude Number 2.5 to 4.5

by NANI G. BHOWMIK

Title: Hydraulic Jump Type Stilling Basins for Froude Number 2.5 to 4.5.

Abstract: Hydraulic jump type stilling basins are used to prevent the detrimental effects of the supercritical flow velocity on the stability of the channel. Laboratory investigations were conducted for both the ordinary and the forced hydraulic jumps on a horizontal floor in the Froude number range of 2.5 to 4.5. Data from the ordinary hydraulic jump correlate well with the theory and other published data. A set of appurtenances (baffle blocks and an end sill, basin L) for forced hydraulic jump was found to perform satisfactorily. Comparison of the test data from this basin with corresponding data from the ordinary hydraulic jump showed that the required tail-water depth can be decreased, energy loss can be increased, and the jump can be formed in a much shorter basin. A theoretical relationship has also been developed to predict the turbulent pressure fluctuations in the stilling basins. Hydraulic design of stilling basins for the Froude number range of 2.5 to 4.5 can be accomplished with the aid of the criteria developed in the report.

Reference: Bhowmik, Nani G. Hydraulic Jump Type Stilling Basins for Froude Number 2.5 to 4.5. Illinois State Water Survey, Urbana, Report of Investigation 67, 1971.

Indexing Terms: Baffles, design criteria, energy losses, Froude number, hydraulic jump, laboratory tests, sluice gates, spillways, stilling basins, tail water, turbulence.

URBANA

1971

Printed by authority of the State of Illinois-Ch. 127, IRS, Par. 58.29

CONTENTS

Hydraulic Jump Type Stilling Basins for Froude Number 2.5 to 4.5

by Nani G. Bhowmik

ABSTRACT

Water flowing at the supercritical stage with very high velocity is detrimental to the stability of the channel. Stilling basins with provisions for dissipating excess amounts of energy are used to prevent the erosion of the channel and to form an efficient hydraulic jump. The hydraulic jump is an extremely useful phenomenon which can be forced to form at the foot of a spillway, canal structure, culvert outlet, or transition structure to reduce the flow velocity with an associated reduction in the energy content of the flow.

Since no satisfactory design criteria existed for stilling basins in the low Froude number range of 2.5 to 4.5, laboratory tests were conducted to investigate the possibilities of increasing the energy loss and shortening the required basin length for this particular range of Froude number. Tests were made in a 2-foot-wide glass walled tilting flume. The hydraulic jumps on the horizontal floor were developed with the aid of a sluice gate. Jumps were forced to form in a particular location by the addition of appurtenances, such as baffle blocks and end sills. The tail-water depth was simulated by controlling the downstream depth with a tailgate in the flume. Data were collected for both the ordinary hydraulic jump and the forced hydraulic jump.

Out of the many different basins and arrangements utilized in the laboratory, a set of appurtenances and geometrical arrangements designed for basin L was found to perform satisfactorily. Comparison of the basin L test data for the forced hydraulic jump with the data from an ordinary hydraulic jump for the same Froude number shows that the energy loss can be increased, the required downstream depth of water can be about 5 percent less than the sequent depth, and the jump can be formed in a much shorter basin.

Some wave activity was found to be present in the stilling basin, and the spill that might occur can be prevented by proper design of freeboard.

All comparisons of the test data were made by computing and plotting the nondimensional ratios as follows: 1) ratio of downstream depth to upstream depth with upstream Froude number, 2) ratio of the energy loss to the incoming energy per pound of fluid with the upstream Froude number, and 3) the ratio of the length of the basin to the sequent depth with the upstream Froude number.

INTRODUCTION

Many stilling basins are of the hydraulic jump type with the jump occurring either on a horizontal floor or on a sloping apron. Sometimes these basins are supplied with appurtenances that increase the overall roughness of the basins. This in turn increases the energy dissipation, decreases the sequent depth, and requires a shorter basin for the full development of the hydraulic jump. In most instances the normal water depth in the downstream section of the channel is not sufficient to form a fully developed hydraulic jump. Stabilization of the jump with increased downstream depth can be attained by deepening the basin, but this may not be economical. The depth of water after the jump is related to the energy content of the flow, and any reduction in energy content with increased energy dissipation in the jump will reduce the required depth of flow after the jump.

Reducing the length of the basin will definitely be economical provided a fully developed hydraulic jump can be formed and contained within a shorter basin. Appurtenances in the basin assist in this by reducing the length of the basin for the particular flow condition.

Stilling basin designs are based primarily on experience, analytical background, laboratory investigations, and model studies. Although model studies may be made for large structures, a detailed model study to establish guidelines for a small structure may not be economical. In such an instance, the designer must depend on experience and rely on other experimental and prototype performances of stilling basins under similar circumstances.

Although design criteria have been established for basins with a high upstream Froude number, no satisfactory design method has existed for stilling basins in the Froude number range of 2.5 to 4.5. The U.S. Bureau of Reclamation (Peterka[1]) terms a hydraulic jump in this range of Froude number as a transition jump with rough water surfaces. Since hydraulic jumps in this range of Froude number are

followed by waves in the downstream channel, some authors[1] have suggested avoiding designing stilling basins in this range if it is physically possible.

Hydraulic jumps in the Froude number range of 2.5 to 4.5 are encountered in canal structures, diversion or low head spillways, and sometimes in culvert outlet works. Therefore, occasionally it is necessary to design a stilling basin to perform at such a low Froude number range. Because of this need, the Illinois State Water Survey decided to perform laboratory investigations on the possibilities of improving the existing design criteria for stilling basins operating at a low Froude number (2.5 to 4.5). The experiments were conducted in the Survey's hydraulic laboratory in a 2-foot-wide glass walled tilting flume and were made for both the ordinary hydraulic jump and for stilling basins supplied with appurtenances such as baffle blocks and end sills. The investigation was carried out on a horizontal basin, in which the supercritical flow was established with the aid of a sluice gate.

Plan of Report

This report is presented in four main sections. The first section provides the methodology used in the investigations, and the second describes the laboratory facilities and procedures for the collection of data.

The third section presents the analysis of the data collected for both the ordinary and the forced hydraulic jump. All the graphical relationships developed for basins A through L are given under this section. A final section summarizes the experiment and the results. Notations for symbols used throughout this report are listed in the back.

Acknowledgments

This study has been conducted by the writer under the general guidance of Harold W. Humphreys, Head of the Hydraulic Systems Section, and the administrative direction of Dr. William C. Ackermann, Chief of the Illinois State Water Survey. The Survey machine shop personnel assisted in the modifications of the flume deemed necessary for the study. John W. Brother, Jr., prepared the illustrations. Thanks are due Mrs. J. Loreena Ivens, Technical Editor, for assistance in editing the final report.

METHODOLOGY

Selection of the basin shape and dimensions is influenced by any one or all of the following factors: absolute size of the structure, frequency of operation, durability of the channel bed downstream from the stilling basin, and the use of chute blocks, baffle blocks, and other appurtenances. Appurtenances help to dissipate some excess energy and to reduce the required length of the basin.

Hydraulic jump action is moved in the upstream portion of the basin with the addition of unstreamlined baffle blocks. The baffle blocks contribute toward the stability of the basin, reduce the wave activity, and prevent sweepout of the jump at an early stage of flow when the tail-water depth is not sufficient for the full development of the jump. With an increase in the value of the Froude number, F_1, some danger exists in possible cavitation damages to the baffle blocks or chute blocks.

In case of a sloping channel when the stilling action takes place in both the sloping and the horizontal apron, chute blocks partially deflect the high velocity jet toward the surface thus assisting in the stability and early formation cf the jump within the basin.

An erodible channel with loose materials in the downstream reach necessitates the reduction of flow velocity after the jump with an appurtenance such as an end sill. The end sill deflects the high velocity jet from the floor of the channel toward the water surface, thus reducing the erosion capability of the flow and at the same time helping to maintain the stability of the bed materials just downstream of the end sill with the formation of eddies directed upstream.

Characteristics of Hydraulic Jump for Froude Number 2.5 to 9.0

Depending upon the supercritical Froude number F_1 of the incoming flow, the formation and other associated characteristics of the jump vary. The U.S. Bureau of Reclamation[1] points out that there are at least four distinct forms of the hydraulic jump that may occur on a horizontal apron, as shown in figure 1.

When the Froude number is between 1.7 and 2.5 (figure 1a), some small rollers develop on the surface but the downstream water surface remains smooth. This jump may be called a weak jump. For the Froude number range of 2.5 to 4.5 (figure 1b) an oscillating jet enters from the bottom and moves to the surface and back to the bottom with no apparent periodicity. These oscillations produce large waves of irregular period which continue downstream with much wave activity. This jump can be termed an oscillating or transition hydraulic jump with very rough water surface. It was recommended,[1] if possible, to redesign the structure so as to avoid the formation of the jump in this particular range of Froude number.

As the Froude number of the incoming flow increases from 4.5 to 9.0 (figure 1c), a good, stable hydraulic jump is formed with the least interference from the variations of the tail-water depth. When the Froude number is greater than 9.0 (figure 1d), a rough, strong, but effective hydraulic jump is formed. It is to be remembered that this division of the types of hydraulic jumps based on Froude number was

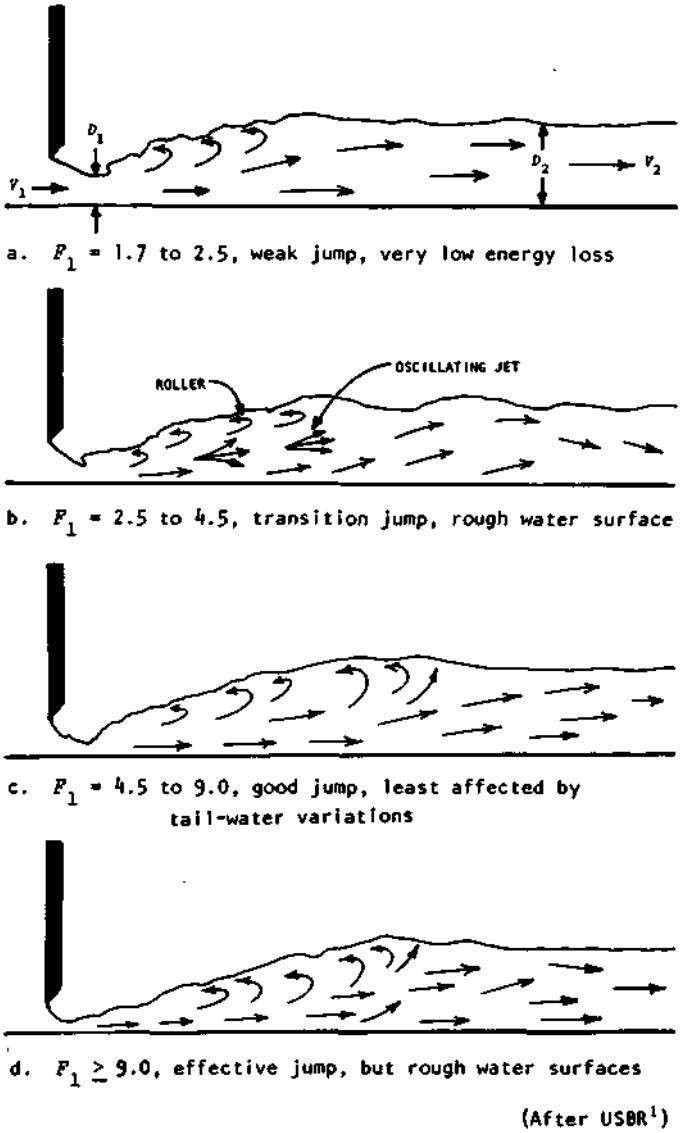

Figure 1. Various forms of the ordinary hydraulic jump

rather arbitrarily made on the basis of experimental investigation. The size, shape, and other characteristics of the structure may also change the formation and stability of the jump at any Froude number.

The U.S. Bureau of Reclamation (USBR[1]) made a few recommendations for the design of stilling basins in the Froude number range of 2.5 to 4.5. From extensive laboratory tests for ogee-shaped spillways with various sizes and arrangements of deflector blocks, guide blocks, and spreader teeth, the **USBR** recommended avoiding too many appurtenances in the basin for this range of Froude number. Excess appurtenances become an obstruction to the flow and thus reduce the effectiveness of the basin. Also, too many appurtenances will create new waves making an already rough surface rougher. **USBR** recommended using only chute blocks and an end sill. Stabilization of the jump with less wave activity required the sequent depth to be increased by 10 percent. The length of the basin needed was equal to the length required for an ordinary hydraulic jump.

St. Anthony Falls Hydraulic Laboratory (Blaisdell[2]) developed a basin called the "SAF stilling basin" primarily for use on small drainage structures such as those built by the U.S. Soil Conservation Service. The range of Froude number to which the design was developed varied from 1.7 to 17. The basin was trapezoidal and had the following pertinent characteristics for a Froude number from 2.5 to 4.5. The ratio of the length of the basin, L, to the sequent depth, D_2, varied from 2.24 to 1.43, the largest being for a Froude number equal to 2.5. Chute blocks, baffle blocks, and an end sill were utilized, and the recommended tail-water depth varied from $1.048D_2$ at Froude number 2.5 to $0.931D_2$ at Froude number 4.5. The total width of the baffle blocks normal to the flow direction was 40 to 55 percent of the total stilling basin width. Effects due to entrained air were neglected in the design.

There are specialized design criteria valid for specific stilling basins. These are generally based on model studies for particular characteristics and flow conditions.

Harleman[3] made an extensive analysis on the effects of baffle blocks on stilling basin performance. A theoretical relationship was developed and laboratory investigations were conducted. It was concluded that the baffle blocks primarily stabilize the jump and reduce the depth required for the formation of the ordinary hydraulic jump. However, compared with an ordinary hydraulic jump, the forced hydraulic jump will have a larger length reduction than depth reduction for similar initial conditions.

Control of the hydraulic jump with vertical sills has also been investigated by Forster and Skrinde,[4] Rand,[5,0] and others. Pillai and Unny[7] investigated the shapes of appurtenances for stilling basin design and concluded that a wedge block with apex angle of 120 degrees performed well under the laboratory flow condition for the Froude number range of 5 to 10.

Ordinary Hydraulic Jump

In the case of an ordinary hydraulic jump, the two independent characteristics are the initial depth D_1 and the initial velocity V_1 at the entrance to the stilling basin. The Froude number associated with the flow entering the stilling basin is

$$F_1 = V_1/\sqrt{gD_1} \qquad (1)$$

Since the energy loss in a hydraulic jump cannot be determined exclusively by the theoretical analysis from the energy relationship, one has to resort to the momentum equation to determine the relationship between D_1, D_2, F_1, and other geometrical properties of the basin. In the analysis it is generally assumed that the boundary shear stress can be neglected, the velocity distribution is uniform[8] before and after the jump, and the pressure distribution is hydrostatic with some variation near the water surface. With these assumptions and from the momentum equation, the relationship between D_2/D_1 and F_1 for a rectangular basin on a horizontal floor is given by

$$D_2/D_1 = \tfrac{1}{2}[(1 + 8F_1^2)^{\frac{1}{2}} - 1] \qquad (2)$$

All the terms in equation 2 were previously defined *(see figure 5 for a sketch of an ordinary hydraulic jump).*

Whenever the boundary roughness is such that the shear stress cannot be neglected, an additional term must appear in equation 2 which in turn will show a decrease in downstream depth for the same upstream depth and Froude number. Rouse[9] in a recent article has shown that in the Bernoulli equation, the total head in a hydraulic jump on a horizontal floor is constant and consists of four parts as follows:

$$H = K + P + S_t + l \qquad (3)$$

where H = total head; K and P are the kinetic energy and piezometric pressure terms given by $K = V^2/2g$ and $P = p/r$; S_t is the transfer of energy through shear to the surrounding fluid (i.e., work done upon the fluid); and l is the head loss of the mean flow through either viscous dissipation or the generation of turbulence. The four quantities shown above must vary in such a manner along a stream line that their sum remains constant at any instant of time. The loss term / in equation 3 can be replaced with the sum of turbulent convection C, diffusion by mixing M, and dissipation e, to give

$$H = K + P + S_t + C + M + \epsilon \qquad (4)$$

Work done by pressure fluctuations and viscous stresses within the eddies is not included in equation 4.

Surface rollers are generated in a hydraulic jump as a result of the presence of noncollinear but equal pressure and dynamic forces. Existence of surface rollers cannot account for all the loss encountered in a hydraulic jump since little energy is lost in the formation of rollers. However, part of this roller is continually torn away and passes downstream as vortices, so that the total energy lost is the summation of all the energies of these vortices. In any real fluid, viscosity brings about the conversion of all these energies into thermal energy. Since the thermal energies cannot be recovered, the hydraulic jump is an irreversible phenomenon.

Profile of the Ordinary Hydraulic jump in a Horizontal Channel

Correct prediction of the profile of a hydraulic jump is desirable in determining the economic design of stilling basin side walls. In most instances ample precautionary measures are taken to confine the jump within the side walls to avoid any damage to the embankment. The knowledge of the profile of the jump in advance will enable the designer to determine the proper height of the side walls. The pressure distribution within the hydraulic jump is not completely hydrostatic, but the pressure profile on the bed corresponds very closely to the water surface profile. Thus, information regarding the jump profile would be very useful in the design of the floor of stilling basins laid on permeable foundations.

Bakhmeteff and Matzke[10] plotted their data on water surface profiles of hydraulic jumps in a dimensionless form with $Y/(D_2 - D_1)$ versus $X/(D_2 - D_1)$ in which X and Y are the dimensional ordinate and abscissa of the profile. The water surfaces did not produce a single profile; rather, they varied depending on the supercritical Froude number. The Froude number varied from 1.98 to 8.63. Rajaratnam and Subramanya[11] were partially successful in collapsing the water surface profiles into a single nondimensional plot by changing the scales of X and Y as a function of $(D_2 - D_1)$. The final empirical relation proposed by Rajaratnam and Subramanya[11] is

$$X/D_1 = 5.08\ F_1 - 7.82 \qquad (5)$$

The shape, nature, energy dissipation characteristics, and geometrical properties of the jump vary according to the Froude number of the incoming flow. Therefore, collapsing the profiles into a single general profile for the Froude number range of 2 to 12 as was done by Rajaratnam and Subramanya[11] is not the proper theoretical approach. Basco[12] has shown that the theoretical approach of Tsubaki[13] predicts the flow profile quite well when compared with the plot of Bakhmeteff and Matzke.[10] However, the theory proposed by Tsubaki[13] is based on an unacceptable assumption of no effect of the roller to the layer equal to a height D_t near the bed. Thus, although equation 5 is not theoretically sound, from a practical consideration, it can be utilized to predict the water surface profile in an ordinary hydraulic jump.

Hydraulic Jump on a Sloping Channel

The present investigation is concerned with the hydraulic jump in a horizontal rectangular basin. Most of the spillways and outlet works are constructed on sloping channels since this is generally dictated by the terrain. The jump forms either on the sloping apron or on the horizontal part of the basin. It is true that the hydraulic jump on a horizontal apron is very sensitive to slight changes in the tail-water depth. However, by increasing the tail-water depth, the jump can be confined within a horizontal basin. The primary consideration for constructing a basin on a sloping apron is structural. The minimum amount of excavation, or the minimum quantity of concrete, or both, for the maximum discharge and available tail-water depth should determine the slope of the apron.

The initial rationale and theoretical analysis of the hydraulic jump problem on a sloping apron was done by Kindsvater.[14] Because of the inclination of the floor, the usual momentum relation for the hydraulic jump contains an additional undetermined term which is to be evaluated from the experimental data.[14] Empirical relationships[1] between several variables for jumps on a sloping apron have also been developed. Most of these relationships are basically derived from experimental results and are designed to be utilized for specific applications. However, it must be pointed out that generalized design procedure cannot be fully de-

veloped for sloping aprons as can be done for horizontal aprons since greater individual judgment is required in the former case.

Forced Hydraulic Jump on a Horizontal Floor

Introduction of different artificial roughnesses, such as chute blocks, baffle blocks, and end sills, in a stilling basin can control the formation of a hydraulic jump at various locations on the apron depending upon the tail-water depth. These artificial roughnesses can forcibly form the jump at the entrance section of the stilling basin and thus confine the jump within a specified limit making it practical to predict the location of the jump. Such a jump can be termed a "forced hydraulic jump." Since a forced hydraulic jump is the basic design element for the hydraulic jump type stilling basin, a considerable amount of experimental, theoretical, and field work has been performed on these types of basins. Blaisdell,[2] Forster and Skrinde,[4] Harleman,[3] Rajaratnam,[15] Peterka,[1] Rand,[5,6] and other investigators have made extensive laboratory experiments, in some instances with field follow-up, on the design and performance of forced hydraulic jump type stilling basins.

The simplest of the appurtenances is a vertical rectangular end sill occupying the whole width of the basin. The vertical sill is ineffective if the sill height is too small or the front of the jump is too far upstream from the end sill. As the Froude number increases, the front of the jump travels downstream, forms a boil above the end sill, and returns to a stage less than critical after the boil; a second hydraulic jump may then develop in the downstream reach of the basin. With further increase in upstream Froude number, the supercritical flow passes over the sill and continues downstream. But for any one of the above cases, adjustment of tail-water depth can substantially alter the location and formation of the jump.

The most common type of stilling basin on a horizontal floor is a rectangular basin supplied with an end sill and one or two rows of baffle blocks which in general are three-dimensional. With some adjustment of the tail-water depth, the hydraulic jump can be stablized within the basin with the aid of baffle blocks and an end sill.

Rand[6] made analyses from laboratory results of the forced hydraulic jump formed 1) below a drop in the channel bottom and 2) with a sluice gate. If a sill of height h is located at a distance L_8 from the toe of the jump, then two extremes are defined: L_{max} which gives a forced jump that is the same as the corresponding ordinary jump, and L_{min} which gives a forced jump a critical height h_c of the end sill or other continuous baffle wall. If L_8 is less than L_{min} or h is less than h_c, the jump moves out of the basin. Rand[6] defined a factor, /, as follows

$$J = (L_s/D_1 - L_{min}/D_1)/(L_{max}/D_1 - L_{min}/D_1) \quad (6)$$

Two graphical relationships were developed, one relating L_8/D_1 with F_1 for the full range of / values and the other relating h_c/D_1 with / for the F_1 range of 2 to 10.

Rajaratnam[8,15] analyzed the forced hydraulic jump phenomenon theoretically by substituting an extra force term in the usual momentum relationship. The force term in the relationship was obtained by inserting a drag force equation due to the presence of the sill with an unknown coefficient of drag. The coefficient of drag C_d was computed for different arrangements of sills and F_1 ranging from 2.5 to 11. A graphical relationship was developed between C_d and the ratio L_8/L_r, where L_r is the length of the roller.

In this connection it must be remembered that the graphical relationship developed between C_d and L_8/L_r is valid only for stilling basins supplied with a solid continuous baffle wall. These stilling basins have very limited practical application since most stilling basins are constructed with baffles and an end sill. Thus the relationship proposed by Rajaratnam[8,15] could not be utilized for the present study.

Effects of Turbulent Pressure Fluctuations on the Stilling Basin

The turbulent pressure fluctuations associated with the turbulent velocity fluctuations in a stilling basin are important not only to design the chute face and chute blocks against uplift but also to indicate the amount and the extent of the cavitation damages that can be expected on the chute block faces. The U.S. Bureau of Reclamation[16] made a laboratory study on the cavitation damages in the chute blocks of stilling basins due to subatmospheric pressures. The critical areas of cavitation damage as reported by USBR[16] were on the sides of the chute blocks near the bottom.

The turbulent pressure fluctuations in the flow associated with the turbulent velocity fluctuations are caused by the intermittent formation and release of eddies in the boundary layer near the channel floor. The eddies thus formed have velocity components which either add to or subtract from the local flow velocity, resulting in velocity fluctuations.

A simple mathematical relationship can be developed to estimate the magnitude of the turbulent pressure fluctuations as a function of the local average velocity head in a stilling basin or in an open channel.[17]

Considering a single point in the flow field near the boundary or any other location in the flow field and writing Bernoulli's equation at any two successive instants of time, one obtains

$$V^2/2g + p/\gamma = (V + v')^2/2g + p'/\gamma \quad (7)$$

where V is the average flow velocity, v' is the instantaneous deviation of flow velocity from the mean, p is the mean pressure associated with mean velocity V, p' is the pressure associated with the velocity $(V + v')$, and y is the specific weight of the fluid. After simplifying, equation 7 becomes

$$p/\gamma - p'/\gamma = \Delta p/\gamma = N(V^2/2g) \quad (8)$$

where

$$N = 2v'/V + (v'/V)^2 = 2(\sigma/V) + (\sigma/V)^2 \quad (9)$$

and $\sigma/V = \sqrt{v'^2}/V$ which is the relative intensity of the turbulence. Equation 9 shows N to be a function of the relative intensity of turbulence σ/V.

Bakhmeteff[18] mentioned that for large streams, σ/V could frequently attain a value of 0.5 to 0.75.

Figure 2, which has been reproduced from reference 19, shows the relative intensity of turbulence a/V plotted against the relative depth y/D, where y is the point in the flow measured above the channel bottom and D is the total channel depth. Figure 2 shows clearly that for open channels the relative intensity of turbulence is a maximum near the bed and decreases toward the surface. This should be particularly true in the case of rough channels where the relative intensity of turbulence near the bed is controlled by the roughness elements present at that location. Therefore, in the case of a stilling basin, the intensity of turbulence can be expected to be a maximum in the vicinity of the roughness elements such as chute blocks.

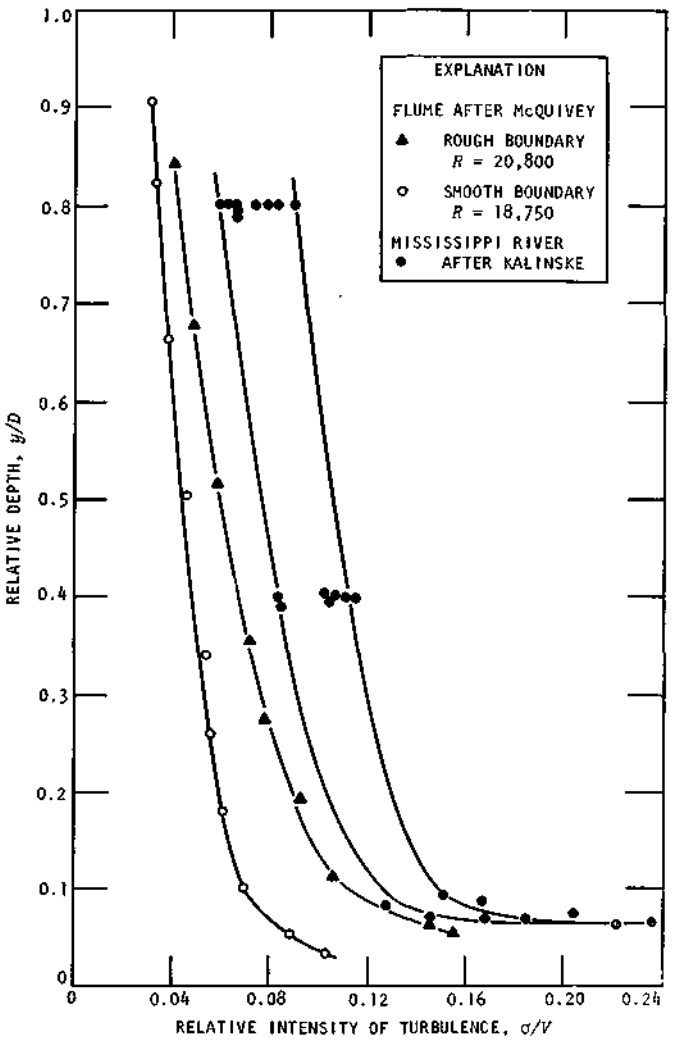

Figure 2. Relative intensity of turbulence for open channel and flume

On the basis of the above derivation, assuming a/V to be approximately equal to 0.25 near the bed and substituting this value in equation 8, one obtains

$$(\Delta p/\gamma)/(V^2/2g) = 0.563 \qquad (10)$$

which indicates that the fluctuating component of the pressure from the mean could easily attain a value equal to about 56 percent of the local average velocity head. Bowers and Tsai[20] have shown from laboratory investigations that the pressure fluctuations in chute blocks can attain a value approximately equal to ± 40 percent of the incident velocity head, where the incident velocity was defined as equal to the velocity at the toe of the jump. Therefore, the average velocity near the chute blocks must be less than the incident velocity, and consequently the fluctuating pressure component near the chute blocks, expressed as a percentage of the local average velocity head, will be greater than ± 40 percent. Thus, the fluctuating pressure component expressed by equation 10 may result in a good approximation of the expected range of pressure fluctuations near the chute blocks in a stilling basin. At this point it must be remembered that the value of the ratio given in equation 10 was obtained on the assumption that σ/V is equal to 0.25. Depending on the measured and/or estimated values of σ/V, the quantity N will change, which in turn will result in a different value of the ratio in equation 10. For example, with a/V = 0.3, the value of the ratio in equation 10 would be 0.69.

Although the method presented here can be utilized to estimate an approximate value of pressure fluctuations, it has been shown[16,20] that the turbulent pressure fluctuations depend on the incident Froude number, tail-water depth, and the discharge.

No data on turbulent pressure fluctuations were collected for the present study. The fluctuating nature of the water surface profile at the low Froude number range of 2.5 to 4.5 makes it extremely difficult to collect any reliable data on turbulent pressure fluctuations.

EXPERIMENTAL PROCEDURE AND DATA COLLECTION

Laboratory Facilities

The laboratory investigation for the present study was conducted in the hydraulic laboratory of the State Water Survey. The main facilities of the laboratory that were used included the 2-foot-wide, 60-foot-long glass walled tilting flume, the laboratory constant head tank and recirculation system, and other pertinent instrumentation. Figure 3 shows the plan and elevation of the 2-foot-wide glass walled flume. A detailed description of the laboratory facilities is given in State Water Survey Circular 48.[21]

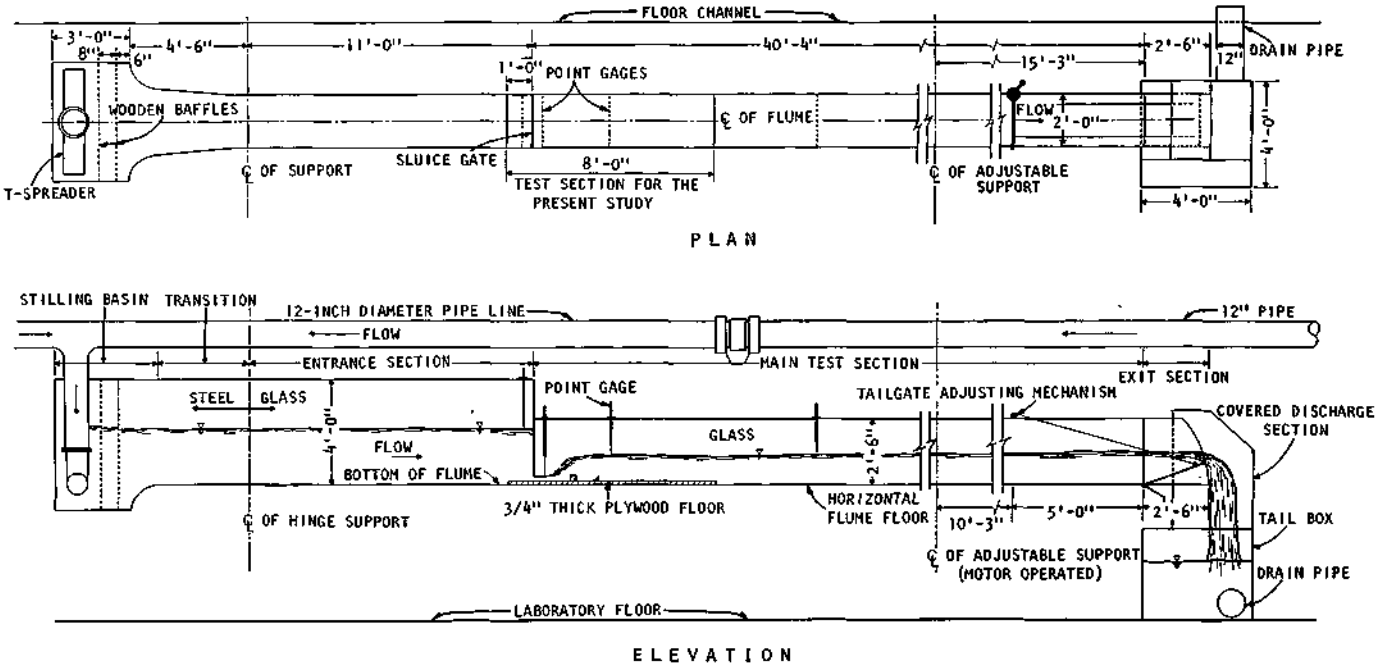

Figure 3. Glass walled tilting flume

The water discharged into the 2-foot-wide flume was measured with the aid of an in-place calibrated short nozzle meter and mercury-water-manometer. The water from the constant head tank was delivered through the 12-inch pipe line into the 4.5-foot-wide head tank of the flume through a T-spreader (figure 3).

Two wooden baffle screens were installed downstream of the T-spreader, as shown in figure 3, to smooth out the disturbances in the flow and to obtain a uniform velocity distribution in the test section. Figure 4 shows the velocity distributions measured 10 feet downstream from the end of the transition before and after the installation of the baffle screens. The point velocities were measured with the aid of a stagnation tube. Figure 4a shows that the vertical velocity distributions before installation of the baffle screens were not uniform and that localized disturbances were present. After the baffle screens were installed, the velocity distribution improved markedly toward uniformity both vertically and laterally (figure 4b). On the basis of these data, the wooden baffle screens were installed in the flume at the locations shown in figure 4c.

In the transition section the width of the flume was gradually reduced to 2 feet which continued to the end of the flume (figure 3). The glass walled entrance section was 4 feet high, 2 feet wide, and 11 feet long. At the end of the entrance section a vertically movable sharp-edged sluice gate was installed. The sluice gate was essential to form the hydraulic jump on a horizontal floor in the downstream section of the flume. The height of the glass walled flume was reduced to 2 feet 6 inches downstream from the sluice gate and this height was maintained to the tailgate. At the test section a sheet of plywood ¾ inch thick, 2 feet wide, and 8 feet long was attached on the floor of the flume (figure 3).

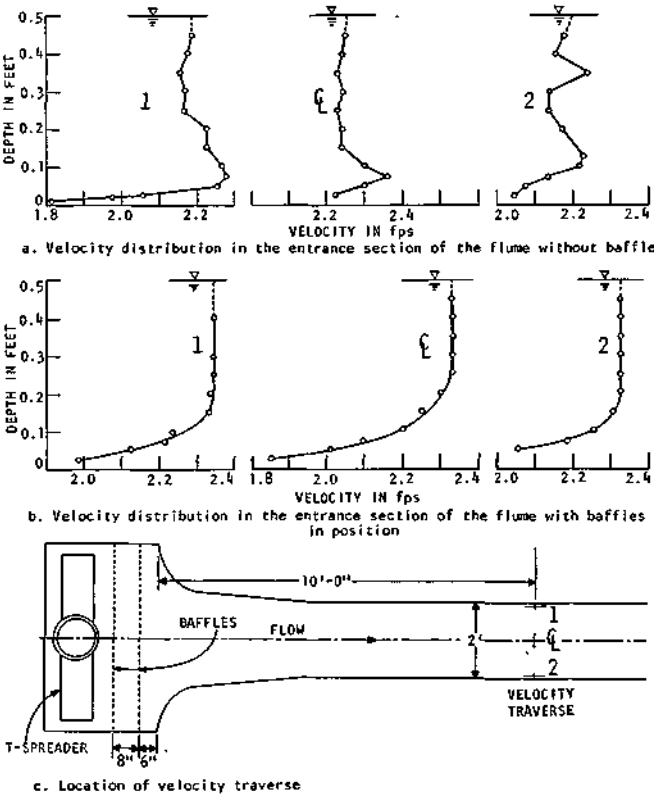

Figure 4. Velocity distribution in the flume entrance section, without baffle piers (a) and with baffles in position (b), and location of velocity traverse (c)

The removal and attachment of various appurtenances was easier on the plywood floor than on a steel floor. Four point gages were utilized to measure the water level (figure 3) and depth of water at various locations. At the downstream end of the flume a movable tailgate was installed which

could be adjusted to obtain any particular depth of flow in the flume.

The flume could be adjusted to obtain an adverse slope of 0.14 percent to a positive slope of 2.5 percent. The adjustment in slopes was accomplished with the aid of a motor (figure 3).

A grid of 0.1 by 0.1 foot was drawn with black marking ink on the outside of the glass wall at the test section. The grid was used to compare the water surface profiles under various flow conditions in the photographs taken to show the performances of the basin.

Data Collection

The general procedures followed for the collection of data were identical for both the ordinary hydraulic jump and the forced hydraulic jump. All the data were collected for a horizontal basin. At the beginning of a run the laboratory constant level tank was filled with water and was allowed to overflow continuously during the experiment. Water discharged into the flume was increased gradually and the sluice gate was adjusted to give the desired depth of flow. As soon as the water level in the flume head tank was sufficient to produce a supercritical flow regime just downstream of the sluice gate, a hydraulic jump would form depending upon the tail-water depth or appurtenances in the stilling basin, or both.

Ordinary Hydraulic Jump

For this case, the tail-water depth was adjusted so that the jump always formed on the plywood floor. Flow discharge, sluice gate opening, and tail-water depth were adjusted for each run to obtain the desired flow condition. An attempt was made to obtain the first set of data for a Froude number value close to 2.5. Then the discharge was increased a small amount and allowed to stabilize before the next set of data was collected. The procedure was repeated for the full range of desired Froude numbers.

The data collected for each of the runs included the discharge, upstream and downstream flow depth, beginning and end of the jump, and the length of the jump. Photographs were taken in some cases, and pertinent notes and comments were recorded. The depth of water was measured with the aid of point gages, and the length of the jump and the beginning of the jump from the sluice gate were measured either from the grid on the outside of the glass wall or from a steel tape fixed to the side of the flume.

Forced Hydraulic Jump

The general procedure for collecting data in this category of hydraulic jump was the same as that for the ordinary hydraulic jump. The main difference was the installation of appurtenances such as an end sill, baffle blocks, or both, on the wooden floor at different locations in various geometrical arrangements. This was done to test and observe the stability and performances of the basins. Selection of end sill and baffle blocks for subsequent basins depended on the performance of the basin under investigation. Tests were conducted with only end sills, with only baffle blocks, and with both the end sill and baffle blocks for the range of F_1 from 2.5 to 4.5. Since all tests were conducted on a horizontal floor with the hydraulic jump forming below a sluice gate, no chute blocks were necessary.

The tailgate was adjusted to obtain the desired tail-water depth. This was necessary to simulate the depression in the basin required in the field to match the sequent depth with the downstream depth of flow. For all runs, sufficient time was allowed to establish the flow and the jump in the basin before any data were collected.

The data collected for each run were: discharge, depth of flow for both upstream and downstream sections, position and distance of the toe of the jump in relation to the baffle blocks or end sill, the apparent end of the jump from visual observation, total length of the basin, and in most cases a photograph of the basin showing the side view and the general performance of the basin.

One controversial item of the data was the selection of the end of the jump. This was fixed according to visual observation as the position where the downstream depth of flow intersected the profile of the hydraulic jump. Although it was observed that this point moves to and fro depending upon the flow condition, the average location was taken to be the end of the jump. In most instances, the profile of the jump became parallel to the floor before reaching the end sill or near the end sill. Thus, the distance from the toe of the jump to the downstream end of the sill was assumed to be the length of the basin.

After one set of data had been collected for a particular flow condition, the discharge was changed, and the flow was allowed to reestablish itself although sometimes it was necessary to adjust the tailgate to increase the downstream depth to obtain a stable hydraulic jump in the basin. The whole procedure was repeated until sufficient data had been collected for the particular basin under consideration. Whenever it was observed that the basin under test was not performing satisfactorily, a different arrangement of appurtenances was tried and enough data were collected to make inferences as to the suitability of the basin for the range of flow conditions. The detailed and separate analysis of the data collected from each of the basins with their associated performances are described in the next section.

ANALYSIS OF THE DATA

This section is in two broad divisions, one for the ordinary hydraulic jump and the other for the forced hydraulic jump. As previously stated, the main objective of this study was to explore the possibilities of increasing the energy loss, decreasing the required tail-water depth, and shortening the length of the basin for the satisfactory performance of the hydraulic jump type stilling basins. Any improvement in the performance of a basin was checked by comparing the different characteristics of the forced hydraulic jump with the corresponding properties of the ordinary hydraulic jump.

In order to check the general overall performance of the basin, data for the ordinary hydraulic jump were collected and compared with other existing data on the ordinary hydraulic jump for a rectangular basin with a horizontal floor. All data collected were expressed in dimensionless form since this is an easy and sensible way to compare data from different basins.

Supercritical depth D_1 and supercritical velocity V_1 are the two independent variables in the hydraulic jump; hence, the supercritical Froude number F_1 is an important variable for comparing the results from various basins. The other dimensionless variables utilized included

$$D_2/D_1, E_L/E_1 \text{ or } E_L/(E_1 - E_c), h_1/D_1, \text{and } h_2/D_1 \quad (11)$$

where E_L is the energy loss and is equal to $E_1 - E_2$ which are the specific energies before and after the jump; E_c is the specific energy associated with the critical depth; and h_1 and h_2 are the heights of the baffle blocks and the end sill, respectively.

Figures 5 and 6 show definition sketches for the ordinary hydraulic jump and the forced hydraulic jump, respectively. The specific energy diagram for both the ordinary and the forced hydraulic jump is shown in figure 7.

Ordinary Hydraulic Jump

The analytical relationship between the depth ratio and the upstream Froude number for a rectangular channel is given by equation 2. The energy loss between the upstream and downstream section of the hydraulic jump is obtained

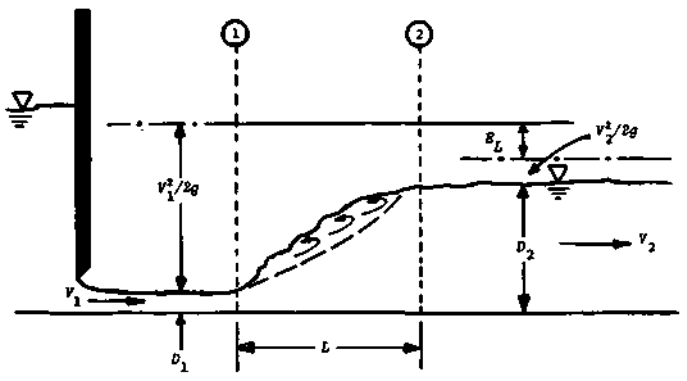

Figure 5. Definition sketch for ordinary hydraulic jump

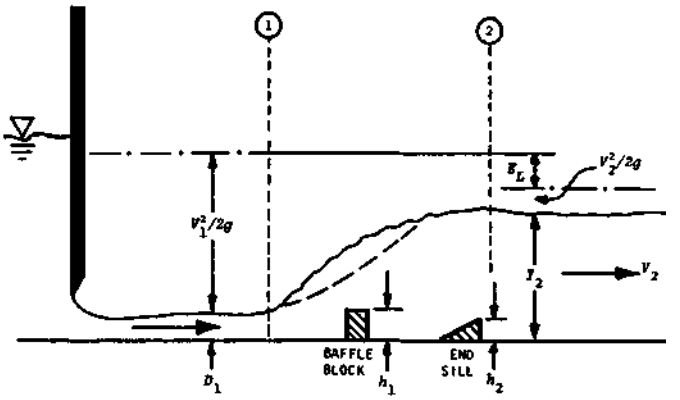

Figure 6. Definition sketch for forced hydraulic jump

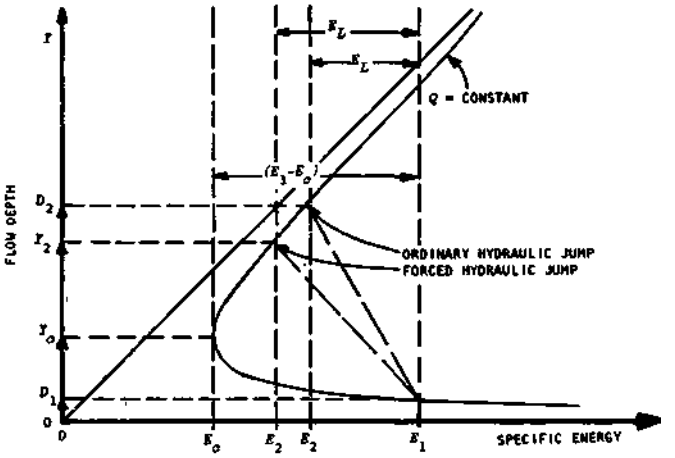

Figure 7. Specific energy diagram for hydraulic jump

by writing the specific energy equation between sections 1 and 2 in figures 5 and 6. The energy loss is given by

$$E_L = (V_1^2/2g + D_1) - (V_2^2/2g + D_2) = E_1 - E_2 \quad (12)$$

Whenever the discharge in a rectangular channel is constant, a definite relationship exists between the depth of flow and the specific energy, as shown in figure 7. The flow attains its minimum specific energy at the critical depth of flow and is given by

$$E_c = V_c^2/2g + Y_c = 1.5\, Y_c \quad (13)$$

where E_c is the specific energy associated with the critical depth of flow and V_c and Y_c are the critical velocity and critical depth, respectively.

Relationship of Depth Ratio and Froude Number

Figure 8 shows the relationship between the depth ratio D_2/D_1 and the Froude number F_1. The theoretical relationship given by equation 2 is also shown. The data plotted are those from the present study, designated as SWS, and the data from USBR flumes E and F as reported by Peterka.[1] Examination of the figure shows that the correlation be-

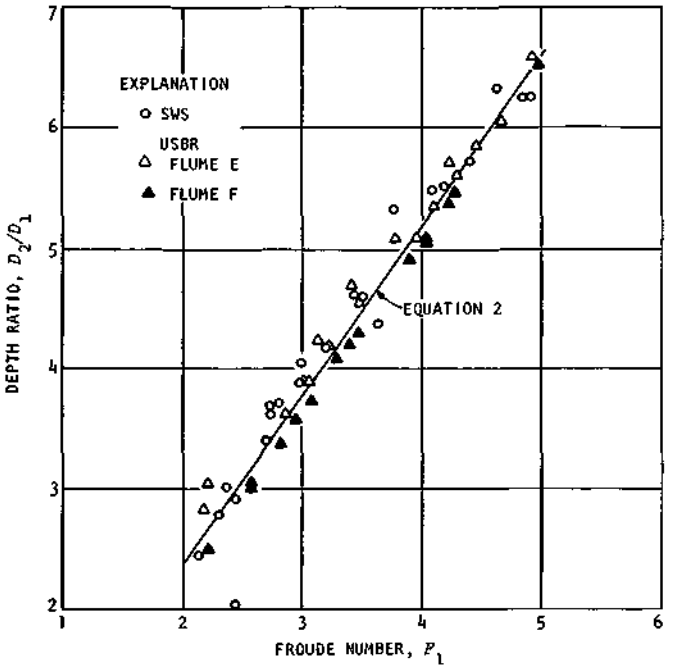

Figure 8. Relationship between depth ratio and Froude number for ordinary hydraulic jump

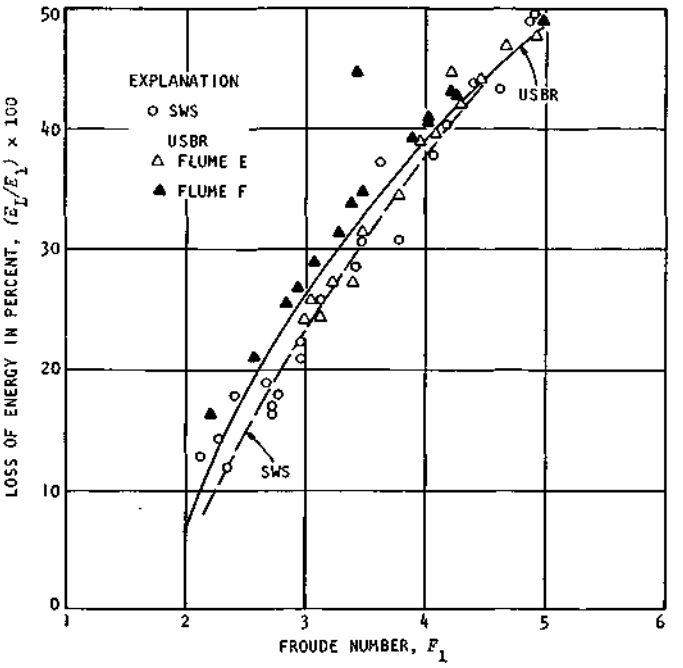

Figure 9. Energy loss in the ordinary hydraulic jump on a horizontal floor

tween the theory and the laboratory experimental data is very good. It must be remembered that the theoretical relationship was developed on the basis of negligible shear stress on the channel floor and side walls. Small variations in the depth measurement would reflect a scattering in the plot so that a perfect match between the theory and the experimental results cannot be expected.

Energy Loss in the jump

The energy loss in a jump can be expressed in a number of ways, such as a plot of E_L/E_1 with F_1, or E_L/D_1 with F_1, or by any other suitable dimensionless variables. Figure 9 shows a plot of E_L/E_1 with F_1 for the range of Froude number under consideration. Data and the average curve suggested by USBR[1] have also been plotted. Figure 9 shows that the data collected in the SWS study fall, in general, slightly below the USBR curve. However, data collected by USBR from flume E fall in the same general vicinity of the SWS data. With some minor variations, the SWS results are in good agreement with those of the Bureau of Reclamation.[1]

Length of the jump

The length of the jump has been defined in different ways, most commonly as 1) the distance from the toe of the jump to the end of the roller, and 2) the distance from the toe of the jump to the point where the tail-water depth is reached. The second definition has been widely accepted. However, some difficulties still arise as to the location of the point where the profile of the jump attains the tail-water depth. It is completely up to the judgment of the individual investigator to decide upon the end of the jump, mainly from visual observation. Therefore, personal differences are bound to occur and good correlation between the data collected by two individuals cannot be fully expected.

Peterka[1] in his extensive study of the hydraulic jump considered the length of the jump to be the distance from the toe of the jump to a point downstream where either the high velocity jet begins to leave the floor or to a point on the surface immediately downstream from the roller, whichever was the longer. In the present study the length of the jump was measured as the distance between the toe of the jump and the point on the water surface where the profile intersects the tail-water depth. The oscillating nature of the jump in this range of Froude number caused some difficulty in the measurement of the length of the jump, but with practice, satisfactory measurements were possible.

Figure 10 shows a plot of L/D_2 versus Froude number F_1 for the range of flow conditions investigated. The top curve shown in the plot is the length curve recommended by USBR[1] and the other two curves are from Bakhmeteff and Matzke[10] and from the SWS study. The Bakhmeteff and Matzke curve shows that a shorter basin is required to form a fully developed hydraulic jump in comparison with that of USBR. Bakhmeteff and Matzke conducted their experiments in a 6-inch-wide flume, which was too narrow to neglect the side wall and shear stress effects. Consequently, as the Froude number increased, the shear stress on the contact surfaces probably played a major role in reducing the length of the basin required for the jump. On the other hand, data collected by USBR[1] were mostly from chute flumes, except flume F, and as such the stream lines were curved before entering the jump section. The data from the SWS study follow a pattern similar to that of USBR but show that a

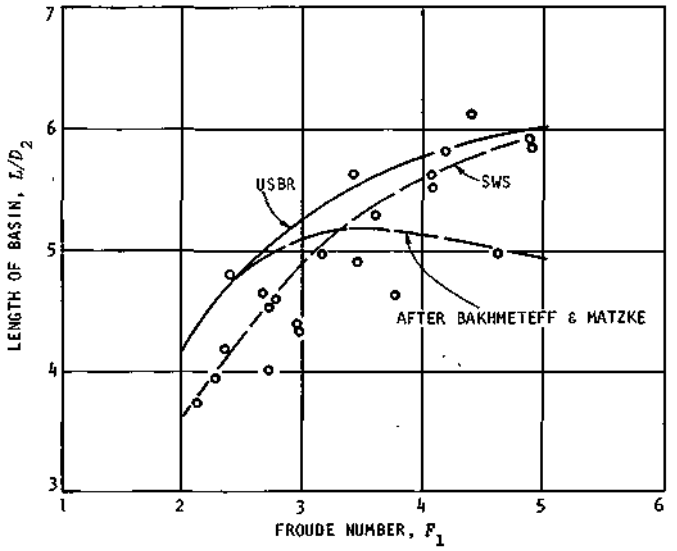

Figure 10. Length of ordinary hydraulic jump in terms of sequent depth

smaller length of the basin is required for the full development of the jump.

The SWS data from basin A for the ordinary hydraulic jump are given in table 1.

Forced Hydraulic Jump

The concerted action of the tail water, baffle blocks, and end sill stabilizes the hydraulic jump on the apron, dissipates much of the energy of the high velocity flow that enters the stilling basin, and can force the jump to form at the entrance section of the basin. The hydraulic jump that is generated as a result of the cumulative efforts of different appurtenances and tail-water depth is termed the "forced hydraulic jump." Experimental investigations on stilling basins equipped with various appurtenances either in combination or individually were conducted and are described below. The tail-water depth Y_2 required to stabilize the forced hydraulic jump was used in the analysis instead of sequent depth D_2.

Tests with Only End Sills

A stilling basin supplied with an end sill, designated here as basin B, is shown in figure 11e. Figure 11 also shows the plot of the water surface profiles with no tail-water adjustment for four F_1 values in basin B. The end sill on the floor of the basin increased the depth of water at that location (figure 11a). This increased depth of water stabilized the hydraulic jump as long as the sequent depth was equal to or less than this depth.

Any increase in the value of F_1 above 2.36 required a higher tail-water depth to stabilize the hydraulic jump at that location. Figures 11b, 11e, and 11d with F_1 equal to 2.81, 3.11, and 3.40, respectively, show that the increased depth of water due to the end sill was insufficient to stabilize the forced hydraulic jump. For these ranges of F_1, the supercritical flow passed over the end sill and continued downstream with some wave activity. The water surface profiles shown in figures 11a through 11d were drawn to scale, and clearly show the wave action in the downstream portion of the basin.

Tests with Only Baffle Blocks

Figure 12 shows basin C which was equipped with only baffle blocks. Experiments were conducted with this basin on a horizontal floor with no tail-water adjustment. The water

Table 1. Test Data for Ordinary Hydraulic Jump, Basin A

Q (cfs)	D_1 (ft)	V_1 (fps)	F_1	E_1 (ft)	D_2 (ft)	E_2 (ft)	$(E_L/E_1) \times 100$	D_2/D_1	L (ft)	L/D_2
0.98	0.1	4.90	2.73	0.471	0.368	0.395	16.12	3.68	1.47	4.00
1.35	0.1	6 75	3.76	0.805	0.531	0.556	30.90	5.31	2.45	4.61
0.98	0.1	4.90	2.73	0.471	0.364	0.392	16.65	3.64	1.64	4.50
1.00	0.1	5.00	2.78	0.487	0.372	0.400	17.85	3.72	1.70	4.57
1.07	0.1	5.35	2.98	0.544	0.404	0.431	20.80	4.04	1.75	4 33
1.14	0.1	5.70	3.18	0.601	0.418	0.447	25.60	4.18	2.18	4.99
1.23	0.1	6.15	3.42	0.687	0.462	0.490	28.60	4.62	2.60	5.62
1.46	0.1	7.30	4.07	0.925	0.549	0.577	37.60	5.49	3.07	5.60
1.66	0.1	8.30	4.62	1.170	0 637	0.663	43.40	6.37	3.15	4.98
0.58	0.1	2 90	1.62	0.230	Waves and undulating water surfaces					
0.64	0.1	3.20	1.78	0.256	Waves and undulating water surfaces					
0.68	0.1	3.40	1.89	0.279	Waves and undulating water surfaces					
0.87	0 1	4.35	2.42	0.393	0.290	0.273	17.6	2.90	1.38	4.76
0.96	0.1	4.80	2.68	0.457	0.340	0.371	18.8	3.40	1.57	4.63
1.06	0.1	5.30	2.96	0.535	0.388	0.417	22.1	3.88	1.70	4.38
1.25	0.1	6.25	3.48	0.701	0.458	0.487	30.5	4.58	2.25	4.90
1.50	0.1	7.50	4.18	0.971	0.552	0.581	40.1	5.52	3.20	5.80
1.76	0.1	8.80	4.90	1.300	0.625	0.655	49.6	6.25	3.65	5.85
1.30	0.1	6.51	3.63	0 755	0.436	0.471	37.6	4.36	2.30	5.27
1.58	0.1	7.90	4.40	1.069	0.571	0.601	43.8	5.71	3.50	6.12
1.75	0.1	8.75	4.87	1.290	0.625	0.655	49.2	6.25	3.70	5.91
0.51	0.077	3.33	2.11	0.249	0.188	0.217	12.8	2.44	0.70	3.73
0.54	0.075	3.57	2.29	0.272	0.209	0.234	14.0	2.79	0.82	3.92
0.55	0.075	3.67	2.35	0.283	0.227	0.250	11.7	3.02	0:95	4.19

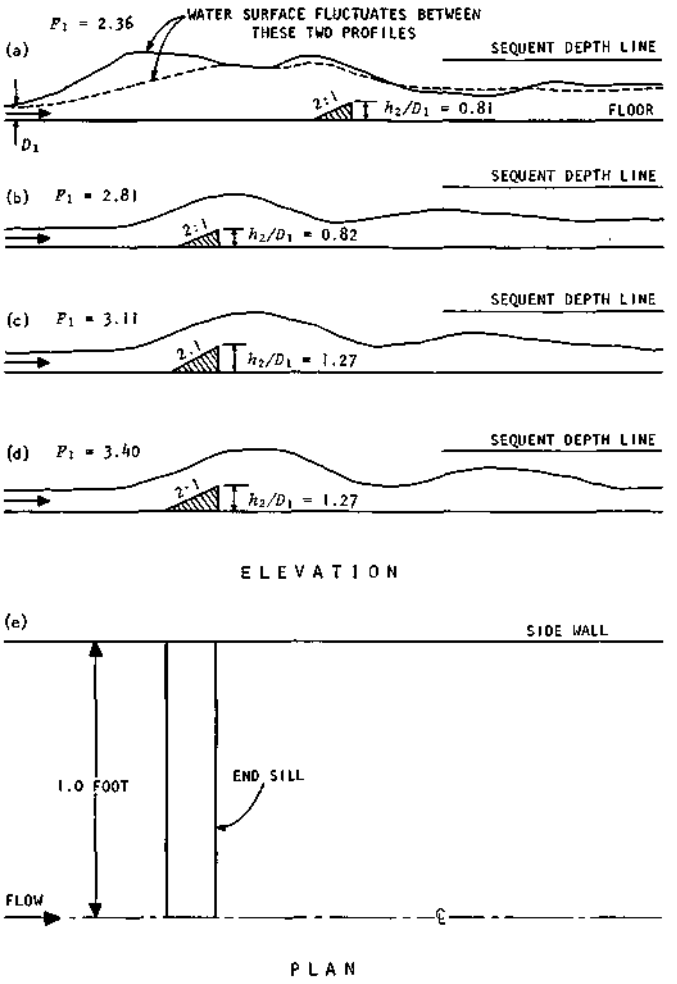

Figure 11. Water surface profiles for basin B, end sill only, no tail-water adjustment

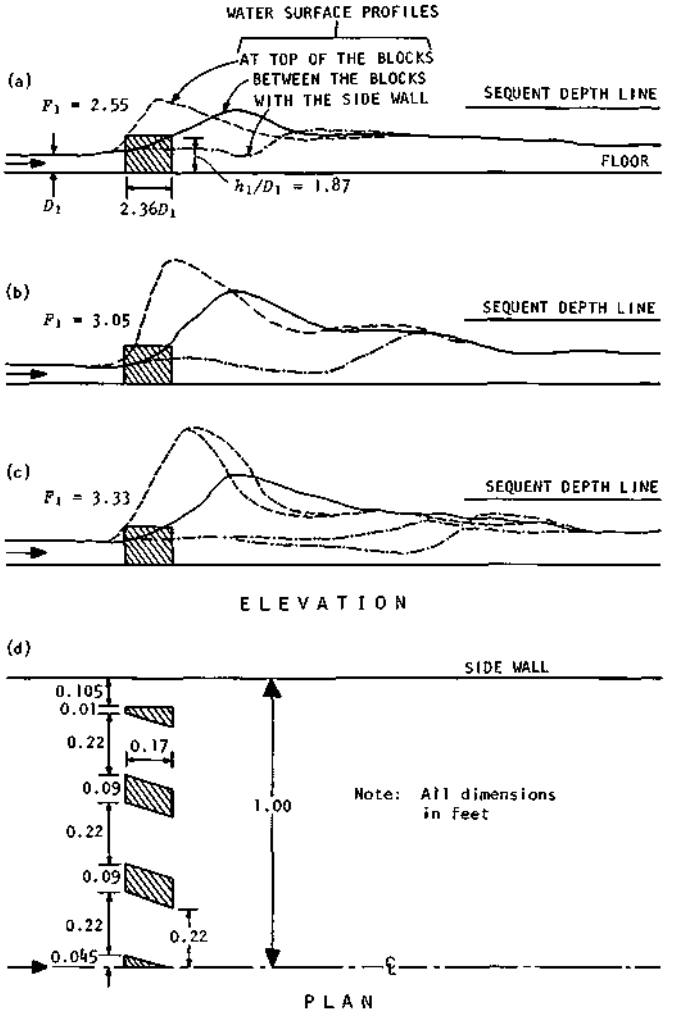

Figure 12. Water surface profiles for basin C, baffle blocks only, no tail-water adjustment

surface profiles were sketched for three distinct variations in the profiles. Since the baffle blocks were not continuous and the presence of spaces between the baffles allowed the high velocity jet at that location to proceed downstream unobstructed, with a slight change in direction, the baffle blocks alone were ineffective in controlling the jump.

At least three different water surface profiles were present in basin C at or near the baffle blocks. Figure 12a shows the three profiles for F_1 equal to 2.55. Water surface profiles both near and at the top of the baffle blocks attained the subcritical flow regime, but returned to the supercritical stage in the downstream portion of the basin. On the other hand, the water surface profile with side walls maintained the supercritical stage with small variations in the depth of water and continued downstream.

With an increase in the F_1 value to 3.05, as shown in figure 12b, the general nature of the profiles remained practically the same as those in figure 12a. However, as the value of F_1 was increased to 3.33, the water surface profile at the top of the baffle blocks started to fluctuate before returning to the supercritical stage in the downstream portion of the basin. There was little fluctuation of the water surface profile between the blocks. However, the water surface profile with the side wall fluctuated between two profiles (figure 12c). All the profiles merged into a single profile in the downstream portion of the basin and continued downstream with a supercritical depth of flow. As the value of F_1 was increased to about 4.5, the shapes of the water surface profiles remained similar to those shown in figure 12c. The arrangement of the baffle blocks utilized in basin C is shown in figure 12d.

Tests with Baffle Blocks and End Sills

Various combinations of baffle blocks and end sills were investigated to explore the general performances of the stilling basin for the range of flow conditions under consideration. As a starting point, the height, width, and slopes of the baffle blocks and end sill were made following the recommendations for basin III by USBR.[1] The marked differences between the USBR basin and that of the SWS study are twofold: 1) the baffle blocks in the SWS study were oriented in such a way that the planes of the sloped sides either converged to a point or met on the centerline of the flume (figures 13a and 13c), whereas the USBR basin III baffle

blocks were rectangular and oriented normal to the direction of flow; 2) the SWS study was conducted on a horizontal floor, but the USBR conducted its experimental investigation on a chute with chute blocks with the flow discharging on a horizontal apron.

For hydraulic jumps at the low Froude number range of 2.5 to 4.5, the distribution of energy in the jump proper is more critical than the additional dissipation or loss of energy resulting from use of appurtenances. Since the addition of appurtenances increases the energy loss by a small margin, the proper and uniform distribution of energy would help to prevent the scouring of the downstream channel and improve the stability of the banks in general. Thus it was anticipated that forcing the high velocity jet to mix near the centerline of the channel would confine the disturbances and the core of the high velocity fluid near the center in the deepest portion of the downstream channel. This was expected to reduce the wave activity close to the banks. The intermixing of jets produces vortices, and as the vortices dissipate as a result of viscous action, thermal energy is produced bringing about the irrecoverable energy loss in the hydraulic jump.

Figures 13, 14, and 15 show the typical basins tested in the laboratory. Some of the basins tested were basically similar, but the orientation and dimensions of the baffles and end sills were varied. A few of the basins are not shown because of their similarity to the basins in figures 13 and 14. Data were collected and evaluated for each of these basins to examine the suitability of the basin for energy dissipation, stability of the jump, and overall performance.

Basin D. Basin D shown in figure 13a was modeled following closely the USBR[1] recommendation for basin III. The projected width of the baffle blocks occupied approximately 69 percent of the width of the flume. The geometrical dimensions of the baffle blocks and end sill were determined according to the curve for basin III. The data collected showed that the improvement of the energy dissipation for the basin was small in comparison with that of the ordinary hydraulic jump. It was observed that the baffle blocks offered excessive obstruction to the flow. The water surface was extremely rough and a small boil was present near the center of the flume.

Figures 16, 17, and 18 show the relationships between F_1 and Y_2/D_1, E_L/E_1, and L/Y_2, respectively. Examination of the figures indicates that the performance of basin D with respect to dissipating energy, reducing the tail-water depth, and shortening the length of the basin was not satisfactory compared with the respective hydraulic properties of the ordinary hydraulic jump. The data collected for basin D are included in table 2.

Basin E. Figure 13b shows the geometrical arrangements of the appurtenances utilized in basin E. Basin E had fewer baffle blocks than basin D and thus obstructed a smaller flow width. Although flow conditions improved to some extent, waves were present in the downstream channel. The hydraulic jumps formed were better than those formed in basin D (figure 13a). The data plotted are shown in figures 16, 17, and 18. Data collected for basin E are given in table 2.

Basin F. The next arrangement tried was that of basin F shown in figure 13c. The oblique arrangements of the baffle blocks were made so that the planes of the longitudinal sides of the baffles converged to a point on the centerline at the downstream side of the end sill. This arrangement was made anticipating a better distribution of the high velocity jet and concentration of the disturbances near the centerline. Tests

Table 2. Test Data for Forced Hydraulic Jump, Basins D and E

Q (cfs)	D_1 (ft)	V_1 (fps)	F_1	E_1 (ft)	Y_2 (ft)	E_2 (ft)	$(E_L/E_1) \times 100$	Y_2/D_1	L (ft)	L/Y_2	Remarks
Basin D $h_1/D_1 = 1.4, h_2/D_1 = 1.3, X/D_1 = 10$											
1.37	0.1	6.85	3.81	0.827	0.365	0.419	49.4	3.65	2.22	6.08	Surface rough
1.45	0.1	7.25	4.05	0.913	0.419	0.465	49.1	4.19	2.23	5.31	Surface rough
1.53	0.1	7.65	4.26	1.001	0.600	0.625	37.5	6.00	2.26	3.77	Surface rough
1.75	0.1	8.75	4.87	1.290	0.620	0.651	49.4	6.20	2 94	4.73	Small undulation
1.43	0.1	7.15	3.98	0.891	0.540	0 567	36.3	5.40	3.04	5.61	Small undulation
1.53	0.1	7.65	4.26	1.001	0.580	0.607	39.3	5.80	3.32	5.71	Small waves
1.87	0.1	9.35	5.21	1.458	0.710	0.737	49.9	7.10	3.35	4.71	Small waves
1.93	0.1	9.66	5.36	1.548	0.710	0.739	52.3	7.10	3.25	4.57	Small waves
2.10	0.1	10.50	5.85	1.810	0.730	0.762	58.0	7.30	3.44	4.71	Small waves
2.23	0.1	11.15	6.21	2 028	0.736	0.771	62.1	7.36	4.00	5.41	Small waves
1.53	0.1	7.65	4.26	1.010	0.520	0.555	45.0	5.20	2.90	5.56	Small waves
1.57	0.1	7.85	4.37	1.054	0.570	0.599	43.2	5.70	3.20	5.61	Small waves
1.63	0.1	8.15	4.54	1.130	0.570	0.619	45.2	5.70	3.06	5.34	Small waves
Basin E $h_1/D_1 = 1.4, h_2/D_1 = 1.3, X/D_1 = 10$											
1.42	0.1	7.10	3.95	0.881	0.486	0.519	41.1	4.86	2.15	4.33	Small waves
1.48	0.1	7.40	4.11	0.950	0.518	0.550	42.1	5.18	2.10	4.06	Small waves
1.56	0.1	7.80	4.34	1.041	0.564	0.594	42.9	5.64	2.50	4.43	Small waves
1.30	0.098	6.50	3.62	0.754	0 460	0.491	34.9	4.60	2.10	4.56	Small waves
1.38	0.098	6.90	3.84	0.838	0.480	0.513	38.8	4.80	2.30	4.79	Small waves
1.47	0.1	7.35	4.09	0.938	0.520	0.551	41.2	5.20	2.25	4.32	Small waves

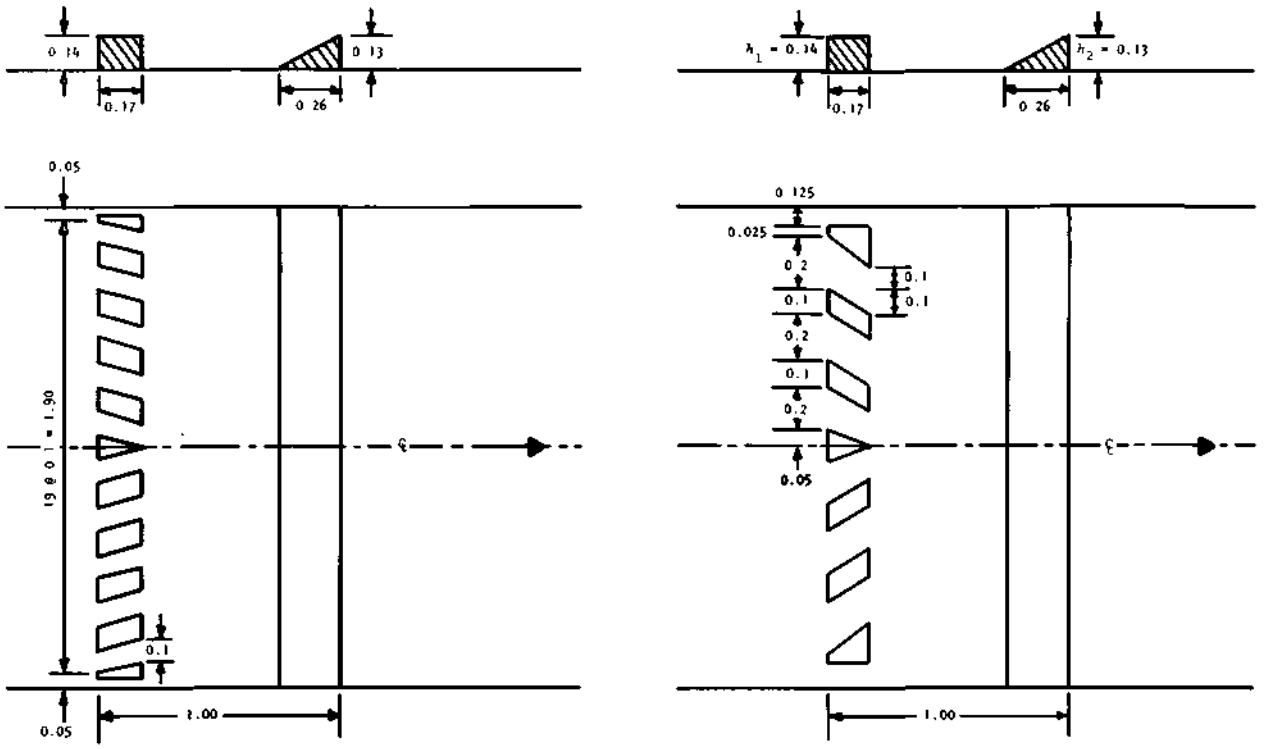

a. Basin D

b. Basin E

Note: All dimensions in feet

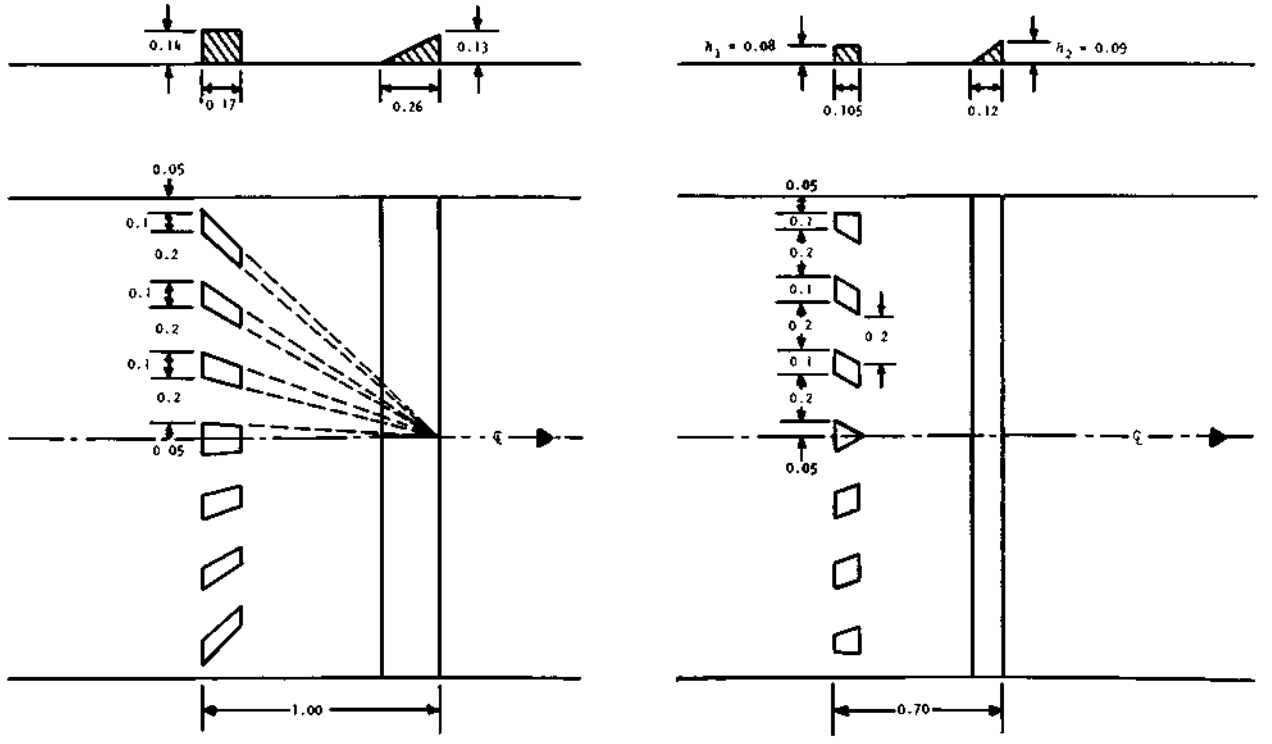

c. Basin F

d. Basin G

Figure 13. Arrangements for basins D, E, F, and G

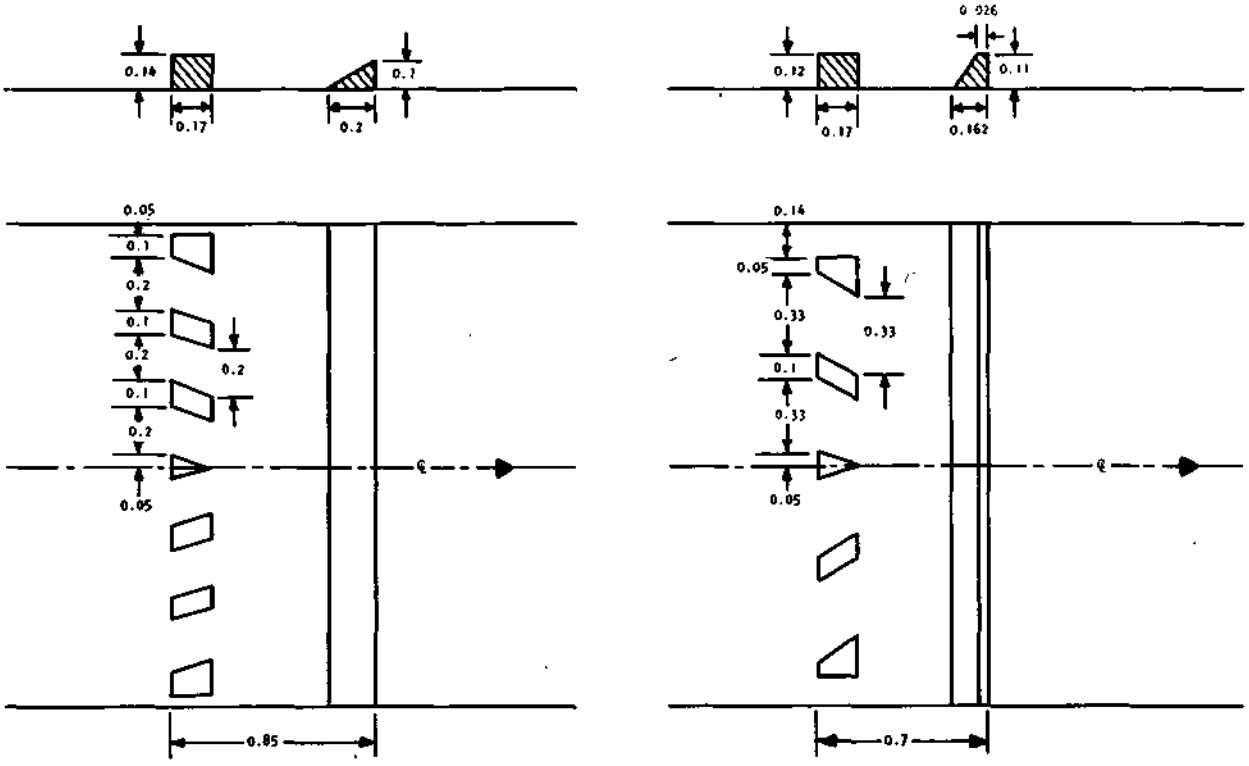

a. Basin H

b. Basin I

Note: All dimensions in feet

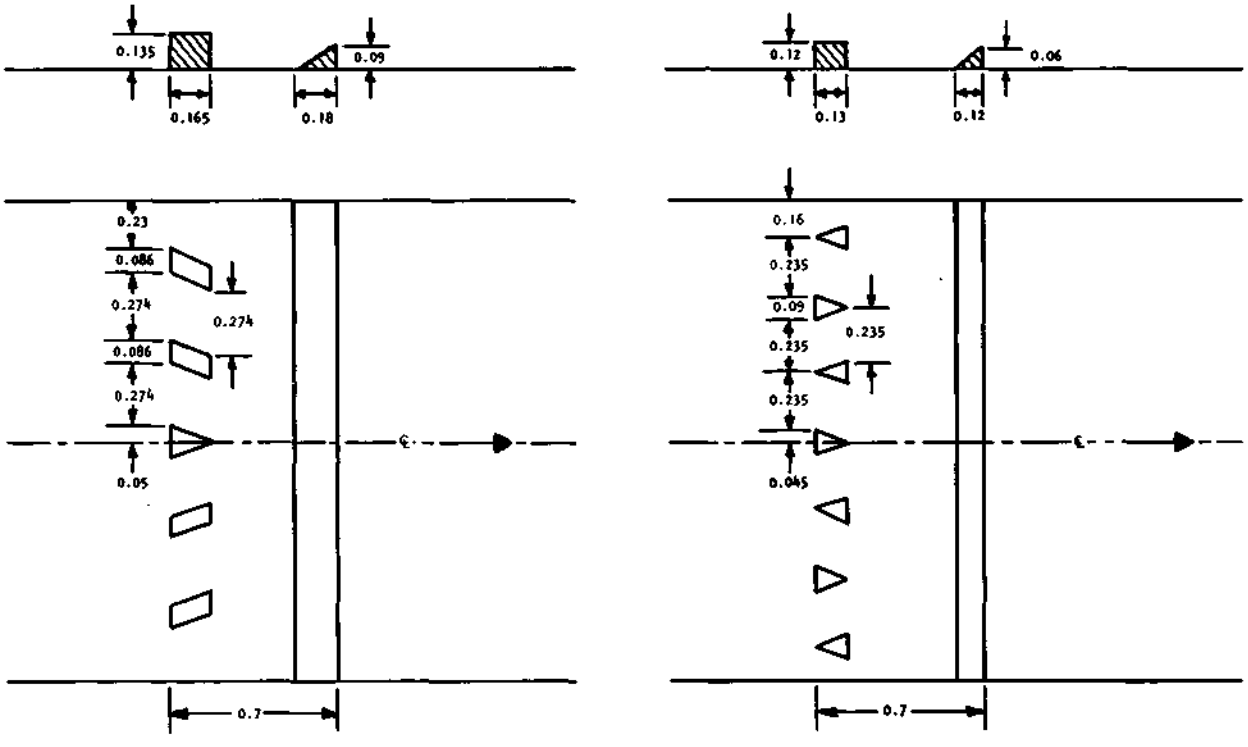

c. Basin J

d. Basin K

Figure 14. Arrangements for basins H, I, J, and K

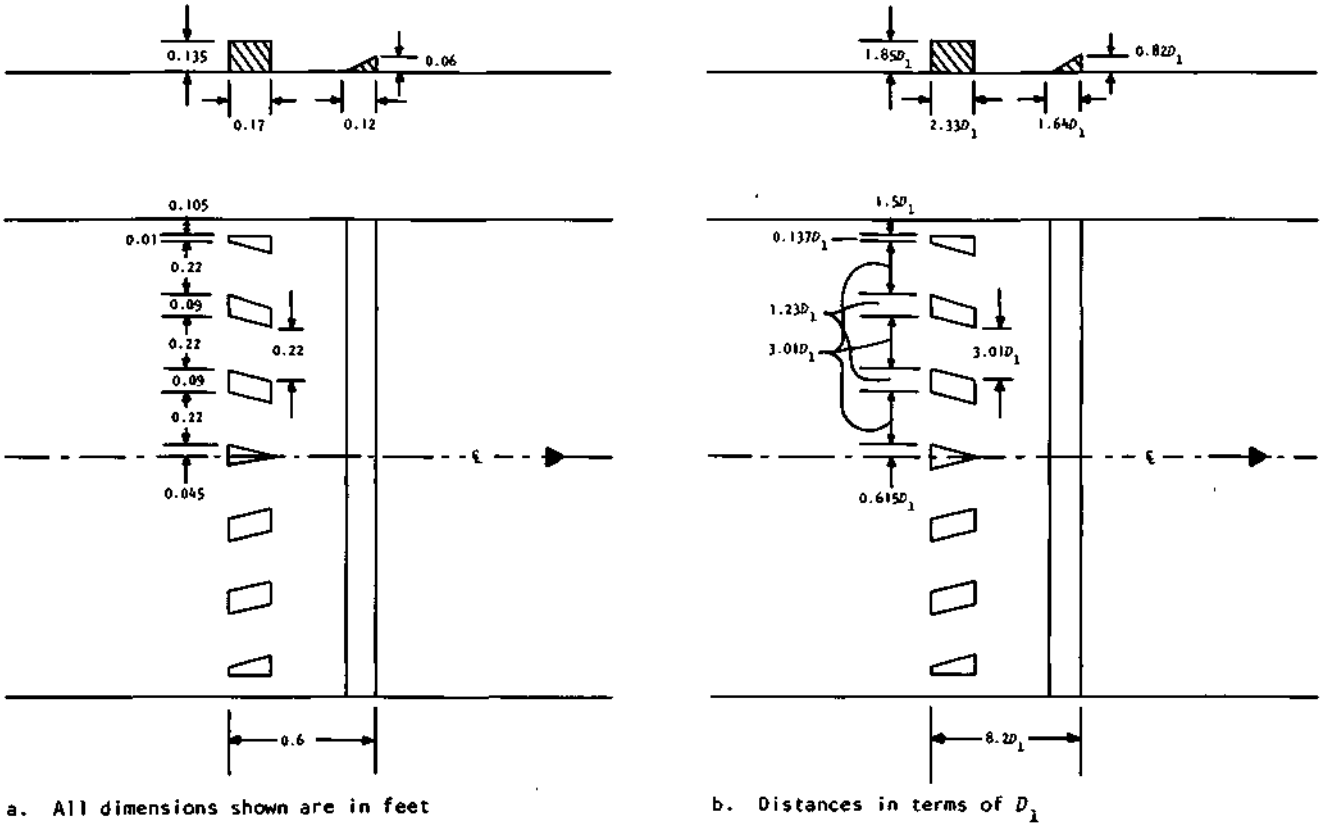

a. All dimensions shown are in feet

b. Distances in terms of D_1

Figure 15. Arrangement for basin L

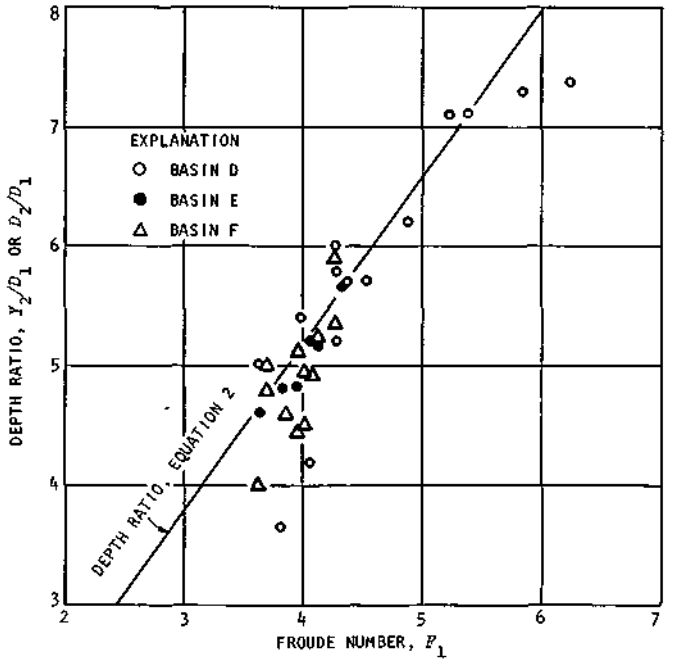

Figure 16. Relationship between depth ratio and Froude number for basins D, E, and F

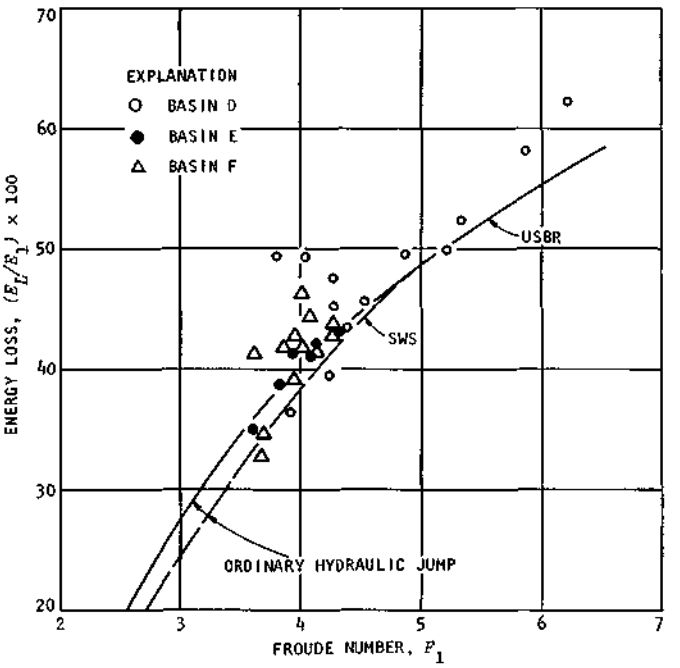

Figure 17. Energy loss in basins D, E, and F

conducted with this arrangement showed that the disturbances and waves produced in the channel were of considerable magnitude and the performance of the basin was not acceptable. Most of the disturbances were generated near the baffle blocks and continued downstream.

In order to investigate the effects of the spacing between the baffles and end sill, this spacing was increased making X / D_1 equal to 15 and tests were conducted. No significant improvement was observed with this arrangement. Then the height of the baffles was reduced $(h_1/D_1 = 1.2)$ and again test data were collected. None of these changes showed any

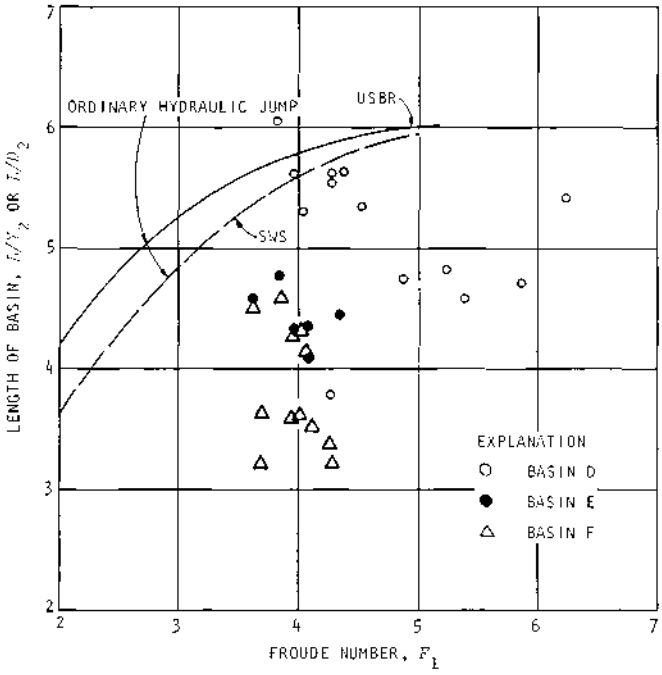

Figure 18. Length ratio for basins D, E, and F

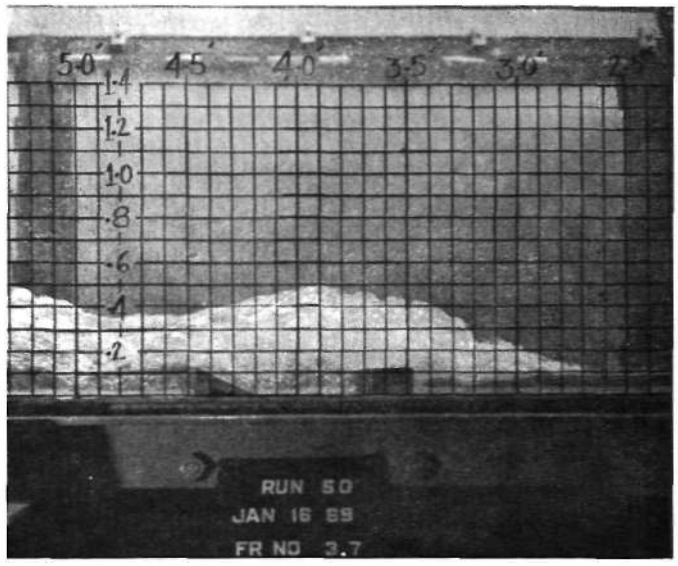

Figure 19. Flow conditions in basin F, Froude number of 3.7

improvement in the basin performance, and this arrangement was abandoned from further consideration. The data collected are plotted in figures 16, 17, and 18. A photograph showing the typical performance of the basin is presented in figure 19. The data collected for basin F are given in table 3.

Basin G. The arrangement of the baffle blocks in basin G, shown in figure 13d, is similar to that of basin E. The end sill utilized had a base to height ratio of 1.33. The distance between the end sill and the baffle blocks was different from that of basin E (an X/D_1 of 9.4, 7, and 12 for basin G and 10 for basin E). The height and base width of the baffle blocks were reduced, but the oblique orientation of the baffle blocks was kept similar to that of basin E. About 50 percent of the width of the flume was occupied by the projected width of the baffles.

With an h_1/D_1 ratio of 0.9 and an X/D_1 ratio of 9.4, the performance of basin G was not satisfactory. High velocity jets passed over the top of the baffles and generated an extensive amount of wave action. The distance between the baffle blocks and the end sill was then reduced making the X/D_1 ratio equal to 7 and the h_1/D_1 ratio equal to 0.8 and tests were conducted. The performance of the basin did not improve, and wave activity was still present in the downstream reach of the flume. In the next set of tests, the upstream depth D_1 was reduced resulting in a higher h_1/D_1 ratio equal to 1.4 and experiments were conducted. This improved the basin performances, but it was observed that the disturbances at or near the baffles close to the side wall were slightly more than those near the centerline. Some wave activity was present in the downstream portion of the chan-

Table 3. Test Data for Forced Hydraulic Jump, Basin F

Q (cfs)	D_1 (ft)	V_1 (fps)	F_1	E_1 (ft)	Y_2 (ft)	E_2 (ft)	$(E_1/E_2) \times 100$	Y_2/D_1	L (ft)	L/Y_2	Remarks
					$h_1/D_1 = 1.4, h_2/D_1 = 1.3, X/D_1 = 10$						
1.30	0.1	6.50	3.62	0.755	0.400	0.441	41.6	4.00	1.80	4.50	Disturbance near the blocks
1.39	0.1	6.95	3.87	0.849	0.459	0.495	41.7	4.59	2.10	4.58	Disturbance near the blocks
1.42	0.1	7.10	3.96	0.880	0.470	0.505	42.6	4.70	2.00	4.26	Disturbance near the blocks
1.45	0.1	7.25	4.03	0.911	0.442	0.484	46.8	4.42	1.90	4.30	Disturbance near the blocks
1.47	0.1	7.35	4.09	0.939	0.490	0.523	44.4	4.90	2.00	4.08	Disturbance near the blocks
					$h_1/D_1 = 1.2, h_2/D_1 = 1.3, X/D_1 = 10$						
1.33	0.1	6.56	3.70	0.779	0.480	0.509	34.5	4.80	1.45	3.20	
1.44	0.1	7.20	4.01	0.903	0.495	0.528	41.6	4.95	1.80	3.64	
1.48	0.1	7.40	4.11	0.950	0.520	0.552	41.9	5.20	1.82	3.50	
1.53	0.1	7.65	4.26	1.090	0.590	0.616	43.6	5.90	1.88	3.19	
1.33	0.1	6.65	3.70	0.782	0.500	0.527	32.6	5.00	1.82	3.65	
1.42	0.1	7.11	3.96	0.887	0.510	0.540	39.1	5.10	1.83	3.59	
1.54	0.1	7.70	4.28	1.020	0.535	0.567	42.7	5.35	1.80	3.36	

nel. The height of the end sill and its relative distance from the baffles seemed to affect the generation of the waves. The performances of the basin were good for the Froude number range of 4 to 5, but as the F_1 value was reduced to 3 or less, waves generated with an increase in the instability of the jump. Thus this arrangement seemed to perform well in the upper range of F_1. Figure 20 shows a typical photograph of the flow condition in basin G for an F_1 value of 3.79 with no adjustment of the tailgate.

Figures 21, 22, and 23 show the relationships for F_1 with Y_2/D_1, E_L/E_1, and L/Y_2, respectively. It can be seen that in comparison with the ordinary hydraulic jump there is some decrease in the ratio of Y_2/D_1, and about 2 to 3 percent increase in the dimensionless energy loss E_L/E_1. The ratio of L/Y_2 decreases with increase in F_1, indicating that as the value of F_1 decreases, a relatively longer basin is required to establish the jump. Figure 24 shows a photograph of the flow condition that existed in basin G for an F_1 value of 3.20. Table 4 shows the test data collected for basin G.

To check the effects of the spacing between the baffle blocks and the end sill with h_1/D_1 = 1.4 and h_2/D_1 = 1.58, the distance between these two sets of appurtenances was

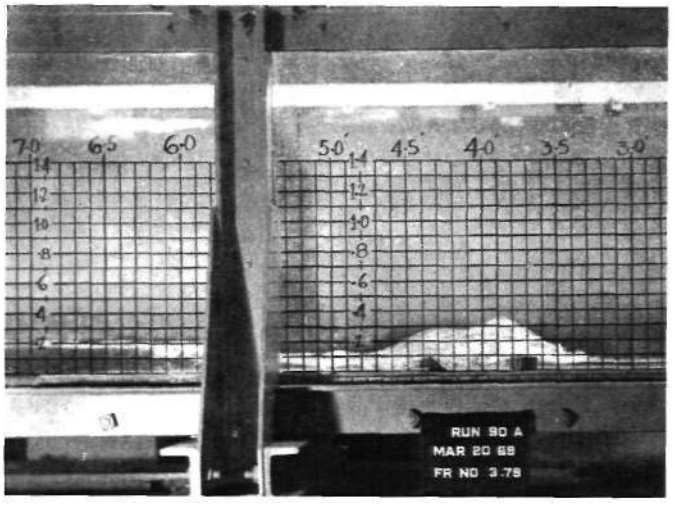

Figure 20. Flow conditions in basin G with no adjustment of the tailgate, Froude number of 3.79

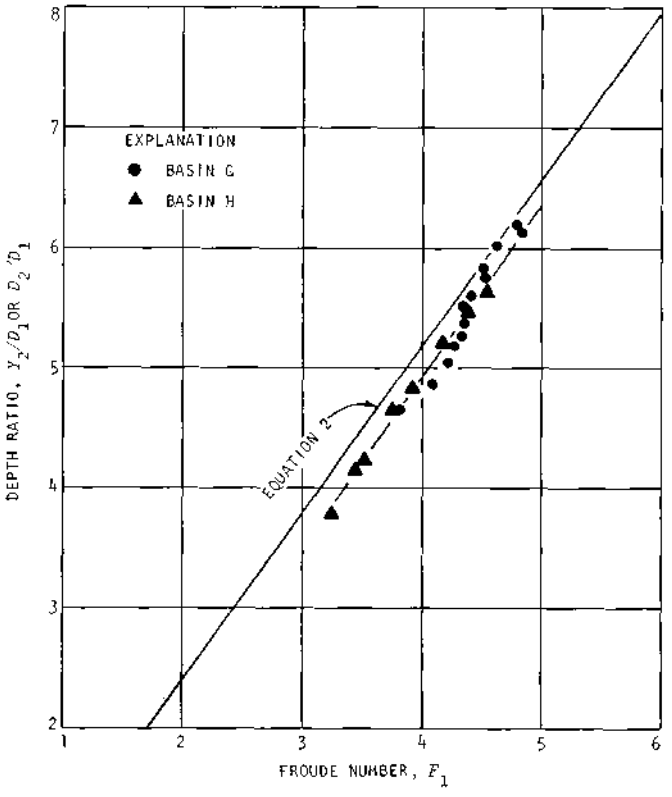

Figure 21. Relationship between depth ratio and Froude number for basins G and H

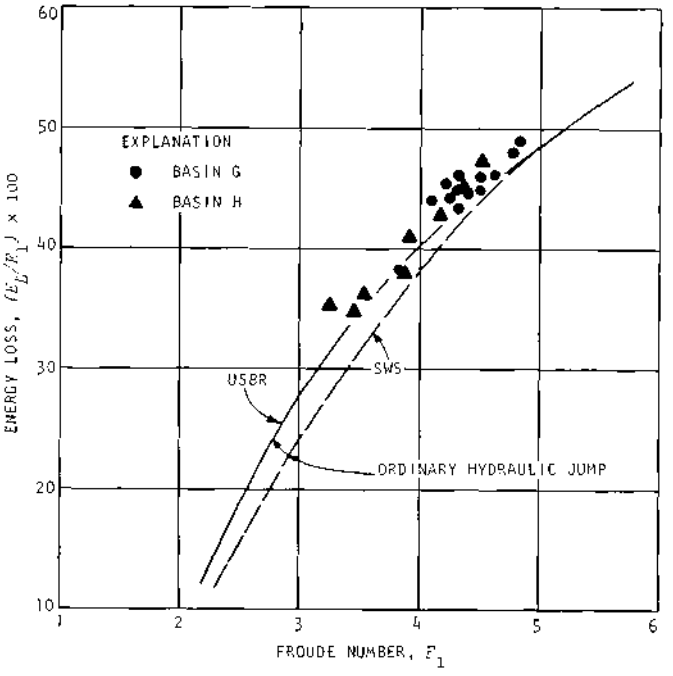

Figure 22. Energy loss in basins G and H

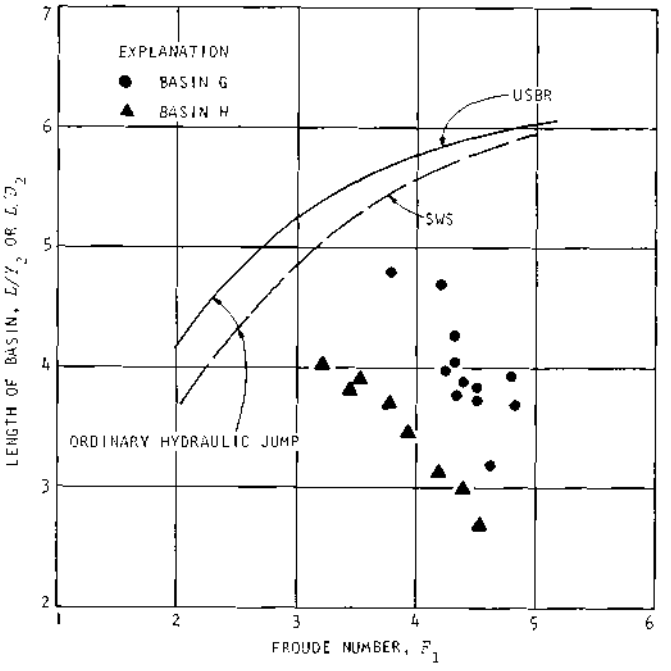

Figure 23. Length ratio for basins G and H

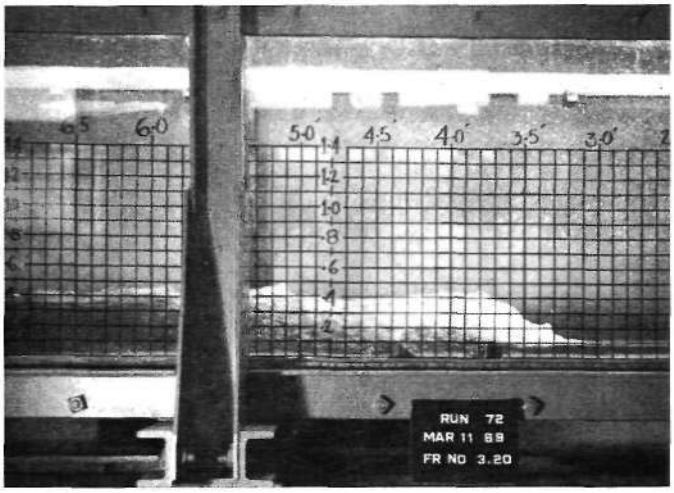

Figure 24. Flow conditions in basin G, Froude number of 3.20

gradually reduced, and test runs were conducted. At about $X/D_1 = 8$, the jump became unstable and the performance of the basin was not satisfactory.

Basin H. Basin H is shown in figure 14a. Basin H was similar to basin E, but the ratio h_2/D_1 was reduced to 1.1 (1.3 for basin E) and the ratio X/D_1 was reduced to 9.3 (10 for basin E). Plots of the data for basin H are shown in figures 21, 22, and 23. It should be noted that, compared with the ordinary hydraulic jump, in basin H 1) Y_2/D_1 for $F_1 = 4.0$ was reduced by about 5 percent, and 2) the increase in energy loss varied from zero to about 3 percent. The ratio of L/Y_2 showed a similar trend to that of basin G with increase in Froude number. However, it appeared that in basin H the jump can be forced to form in a shorter basin than in basin G. The data collected for basin H is shown in table 5.

Some wave activities were present for the whole range of Froude number. The intensity of wave action increased with F_1 equal to or less than 3.3. Figure 25 shows typical performances of the basin. With no tail-water adjustment (figure 25a, $F_1 = 2.96$), a second hydraulic jump was formed in the downstream part of the flume. The generation and propagation of the waves are clearly visible in figure 25b, $F_1 = 3.25$. With increase in the value of the Froude number, the performance of basin H improved, as shown in figure 25c.

The overall performance of basin H was an improvement in comparison with the performances of basins D, E, F, and G. From the demonstrated performance of basin H, and also from visual observation, it was concluded that a basin similar to basins G and H should, with some modifications, perform satisfactorily for the range of Froude number under consideration.

In subsequent test runs, the height of the end sill was reduced to $h_2/D_1 = 0.89$, but no significant improvement in reduction in waves was observed and waves were still present at the lower range of Froude number. Increasing or decreasing the distance between the baffles and end sill did not improve the performance of the basin in comparison with that for the initial geometry of basin H.

Table 4. Test Data for Forced Hydraulic Jump, Basin G

Q (cfs)	D_1 (ft)	V_1 (fps)	F_1	E_1 (ft)	Y_2 (ft)	E_2 (ft)	$(E_1/E_1) \times 100$	Y_2/D_1	L (ft)	L/Y_2
				$h_1/D_1 = 0.9$, $h_2/D_1 = 1.0$, $X/D_1 = 9.4$						
1.27	0.09	7.05	4.13							
1.05	0.09	5.84	3.42							
1.12	0.09	6.21	3.64							
1.15	0.09	6.39	3.75	All tests unsatisfactory						
1.13	0.088	6.41	3.81							
1.18	0.091	6.48	3.78							
				$h_1/D_1 = 0.8$, $h_2/D_1 = 0.9$, $X/D_1 = 7.0$						
1.15	0.1	5.75	3.20							
1.29	0.1	6.45	3.60							
1.47	0.1	7.35	4.07							
1.50	0.1	7.50	4.17	All tests unsatisfactory						
1.56	0.1	7.80	4.34							
1.61	0.1	8.00	4.46							
1.66	0.1	8.30	4.62							
1.68	0.1	8.40	4.67							
				$h_1/D_1 = 1.4$, $h_2/D_1 = 1.58$, $X/D_1 = 12.0$						
0.63	0.057	5.53	4.07	0.531	0.277	0.297	44.0	4.86		
0.63	0.056	5.65	4.20	0.541	0.283	0.302	46.1	5.05	1.30	4.68
0.64	0.056	5.71	4.25	0.561	0.290	0.313	44.3	5.17	1.15	3.96
0.65	0.056	5.81	4.31	0.579	0.294	0.314	45.8	5.25	1.25	4.25
0.67	0.057	5.86	4.33	0.588	0.307	0.326	44.7	5.38	1.15	3.75
0.70	0.057	6.12	4.50	0.637	0.328	0.346	45.7	5.75	1.22	3.72
0.72	0.056	6.43	4.77	0.696	0.346	0.363	47.8	6.19	1.35	3.91
0.75	0.060	6.25	4.50	0.664	0.349	0.367	44.8	5.81	1.33	3.81
0.77	0.060	6.42	4.62	0.700	0.361	0.379	45.9	6.01	1.15	3.19
0.72	0.060	6.00	4.32	0.615	0.336	0.349	43.3	5.50	1.35	4.02
0.57	0.056	5.11	3.79	0.461	No tail-water adjustment					
0.57	0.056	5.11	3.79	0.461	0.262	0.281	38.0	4.68	1.25	4.76
0.64	0.055	5.86	4.40	0.587	0.309	0.326	44.5	5.61	1.20	3.88
0.71	0.055	6.42	4.82	0.693	0.338	0.355	48.8	6.14	1.25	3.60

Basin I. Figure 14b shows basin I in which five baffle blocks and an end sill were utilized. The end sill had a sloped upstream side and horizontal top near the downstream side. Tests were conducted for the Froude number range of approximately 2.5 to 4.5.

It was found that the disturbances near the baffles were reduced, but wave activity was present in the downstream channel and the tail-water depth required to stabilize the jump was relatively more than that required for basin H. Figure 26 shows a photograph of basin I for F_1 equal to 3.7. It is to be noted that water starts to accelerate right after the end sill, accompanied by a decrease in depth and the development and propagation of waves in the downstream direction.

In the next set of tests with basin I, the end sill height ratio h_2/D_1 was changed from 1.25 to 1.01 and the base width from 1.78 to $2(h_2/D_1)$. Test data did not show any marked variation in the performance of the basin in comparison with that for the original geometry of basin I. A typical photograph of the modified basin I with very little tail-water adjustment is given in figure 27. A second hydraulic jump was formed in the downstream portion of the flume and a slight increase in the tail-water depth moved the toe of the jump in the upstream direction. The upstream Froude number for this particular run was 2.73.

Basin J. The arrangement of the appurtenances utilized in basin J is shown in figure 14c. Basin J is similar to basin I, both being equipped with five baffle blocks and an end sill. However, for basin J, the plane of the longitudinal sides of the baffle blocks from both sides of the centerline intersected

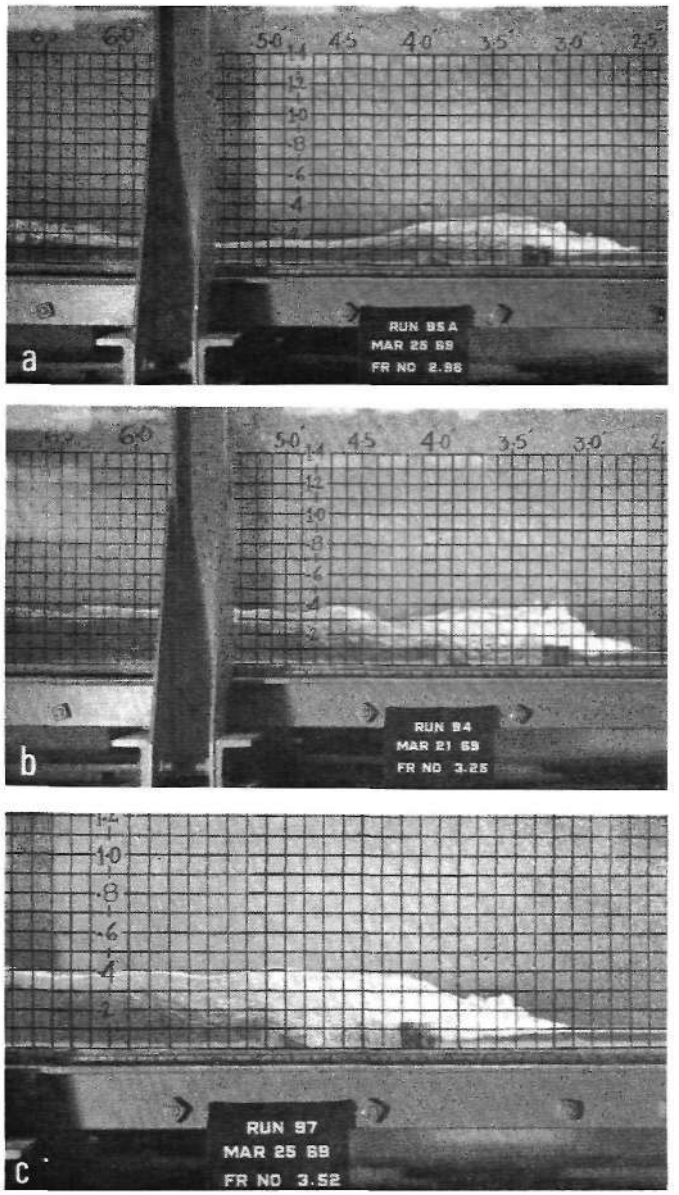

Figure 25. Flow conditions in basin H, showing conditions with no tail-water adjustment (a), waves generated in the basin (b), and improved condition at higher Froude number (c)

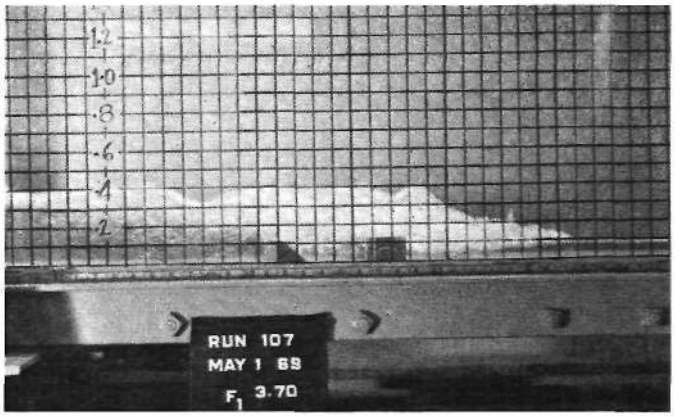

Figure 26. Flow conditions in basin I showing development and propagation of waves, Froude number of 3.70

Table 5. Test Data for Forced Hydraulic Jump, Basin H

Q (cfs)	D_1 (ft)	V_1 (fps)	F_1	E_1 (ft)	Y_2 (ft)	E_2 (ft)	$(E_1/E_1) \times 100$	Y_2/D_1	L (ft)	L/Y_2
				$h_1/D_1 = 1.54$, $h_2/D_1 = 1.1$, $X/D_1 = 9.3$						
0.88	0.090	4.89	2.87	0.459	Waves					
0.99	0.089	5.57	3.25	0.570	0.336	0.370	35.2	3.78	1.35	4.01
0.89	0.089	5.00	2.96	0.476	Waves					
1.08	0.091	5.92	3.46	0.632	0.379	0.414	34.6	4.16	1.45	3.82
1.10	0.091	6.03	3.52	0.652	0.385	0.417	36.1	4.22	1.50	3.90
1.15	0.090	6.40	3.76	0.725	0.420	0.449	37.9	4.66	1.55	3.69
1.21	0.090	6.71	3.93	0.788	0.435	0.465	41.0	4.83	1.50	3.45
1.32	0.089	7.41	4.37	0.939	0.488	0.516	45.0	5.47	1.45	2.98
1.37	0.089	7.70	4.54	1.008	0.503	0.532	47.2	5.65	1.35	2.69
1.26	0.089	7.06	4.17	0.862	0.466	0.494	42.6	5.24	1.45	3.11

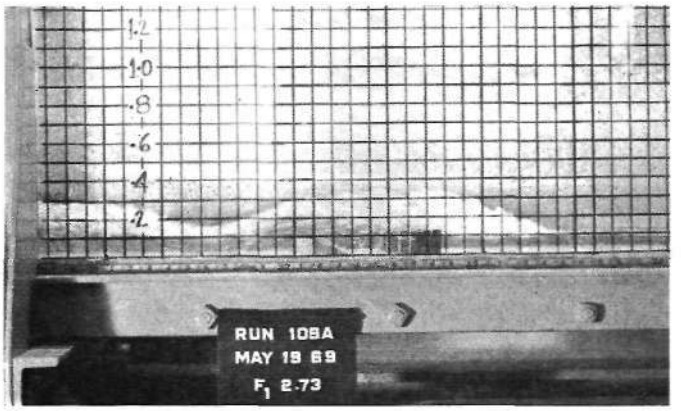

Figure 27. Flow conditions in modified basin I with very little tail-water adjustment, Froude number of 2.73

at the centerline, whereas for basin I the side wall of the flume and the nearest longitudinal side of the baffle block were parallel.

Test results, when compared with the ordinary hydraulic jump, showed no improvement in the performance of the basin. Waves were generated near the side wall and continued downstream. On the basis of these results, stilling basins equipped with five baffle blocks and an end sill were abandoned from further consideration.

Basin K. Basin K is shown in figure 14d. The shape and arrangement of the baffles for this basin arc completely different from those of basins D-J. The adjacent baffles were arranged with opposite orientation to force the intermixing of the high velocity jets. It was expected that the forced mixing of the jets would dissipate some extra energy, distribute the energy content, and stabilize the jump in a shorter basin. Two different end sills were utilized, and the distances between the baffles and the end sill were also varied.

The characteristics of the basin in the first test were: h_1/D_1= 1.71, h_2/D_1= 1.14, X/D_1 = 10, and the base width of the end sill was twice the height of the end sill. Approximately 31.5 percent of the width of the flume was blocked by the baffle blocks. The data collected showed that some waves were generated and continued in the downstream direction. It was felt that the height of the end sill was in fact accelerating the formation of the waves. To test this hypothesis, the height of the end sill was reduced so that the basin characteristics were h_1/D_1 = 1.66, h_2/D_1 = 0.833, and X/D_1 = 9.7. The basin did not perform as well as expected. Waxes were generated near the baffles and continued downstream. Some to-and-fro movement of the toe of the jump was observed. The jump seemed to be unstable at a lower F_1 value around 2.7, but as this value increased to about 4.5. the performance of the basin improved. With an upstream Froude number of approximately 2.5. the location of the jump was quite sensitive to small variations in the tail-water depth.

The next set of data was collected with basin K modified so that h_1/D_1 = 1.64, h_2/D_1 = 0.82, and X/D_1 = 6.90. The major change was that the distance between the baffles and the end sill was shortened, along with a minor increase of about 1.4 percent in the upstream depth. The performance of the basin with this modification did not show much improvement. In fact, for the shorter distance between the end sill and the baffles, wave activity increased and the instability of the jump became more pronounced. It became quite apparent, on the basis of performances of basins D through K, that X/D_1 should lie in between 8.0 and 9.0, probably close to 8.5.

The relationship between the depth ratio Y_2/D_1 and F_1 for basin K is shown in figure 28. Two sets of data, for X/D_1 of 9.7 and 6.9, are plotted in the figure. With the distance between the baffles and the end sill at X/D_1 = 9.7, the tail-water depth required for the higher Froude numbers is less than that needed for the ordinary hydraulic jump. With a Froude number close to 3, there is no appreciable difference between the tail-water depth requirement and the sequent depth for the same F_1. For X/D_1 = 6.9, no significant difference is apparent between the tail-water depth required and the sequent depth.

Figure 29 shows a plot relating energy loss expressed in percent of E_L/E_1 with F_1 for basin K. This plot also indicates that as the spacing (X/D_1) between the baffles and the end sill is increased to 9.7, the energy loss increases over those for the ordinary hydraulic jump shown by USBR and SWS. This is particularly true for higher Froude numbers. On the other hand, with a Froude number of 3, the energv loss for the forced hydraulic jump is practically the same as that for the ordinary jump shown by USBR.

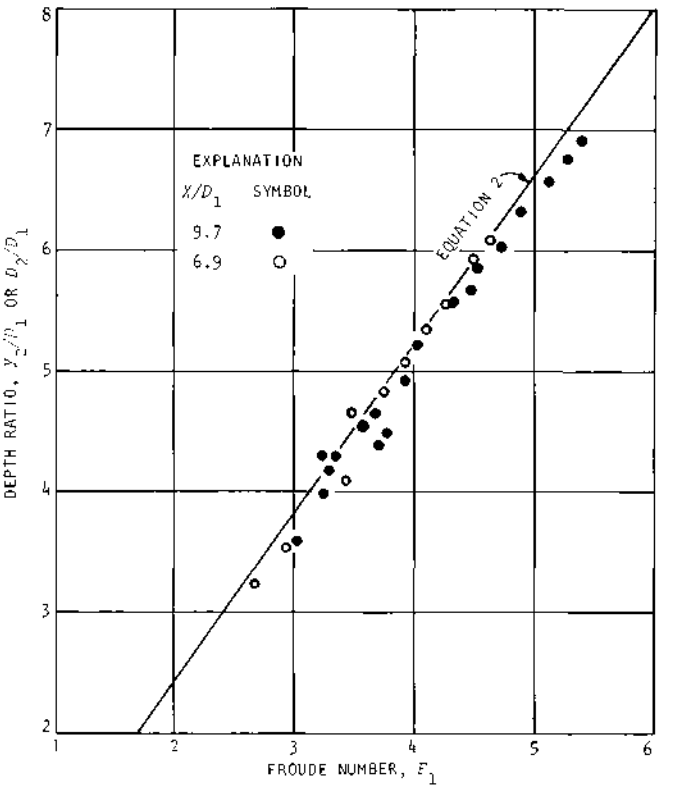

Figure 28. Relationship between depth ratio and Froude number for basin K

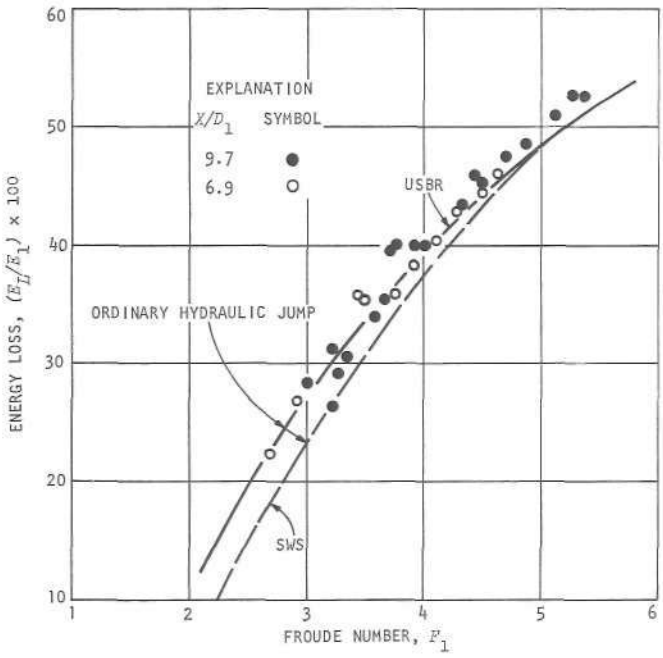

Figure 29. Energy loss in basin K

As the spacing between the end sill and baffles was shortened to X/D_1 = 6.9, the loss of energy for the forced hydraulic jump is practically the same as that of the USBR ordinary jump curve. This again indicates that the spacing of baffles and end sill is an important consideration in the design of stilling basins. However, comparison of the energy losses for both arrangements of basin K with that of the ordinary hydraulic jump from the SWS study shows extra energy loss for the forced hydraulic jump.

The relative length of the basin L/Y_2 is plotted against F_1 in figure 30. As the Froude number increases, the length ratio required with basin K decreases. This may be explained in part by the oscillating nature of the jump at a Froude number close to 2.5. At this low Froude number, the formation of the jump is transitional and requires a tail-water depth close to the sequent depth and a relatively longer basin length for full stability. As the value of F_1 increases, the transitional nature of the jump begins to disappear. Appurtenances can then prevent the sweepout of the jump, and proper adjustment of downstream depth can stabilize the jump in a shorter basin. Figure 30 shows that the length of the basin required follows a similar trend for both arrangements of basin K.

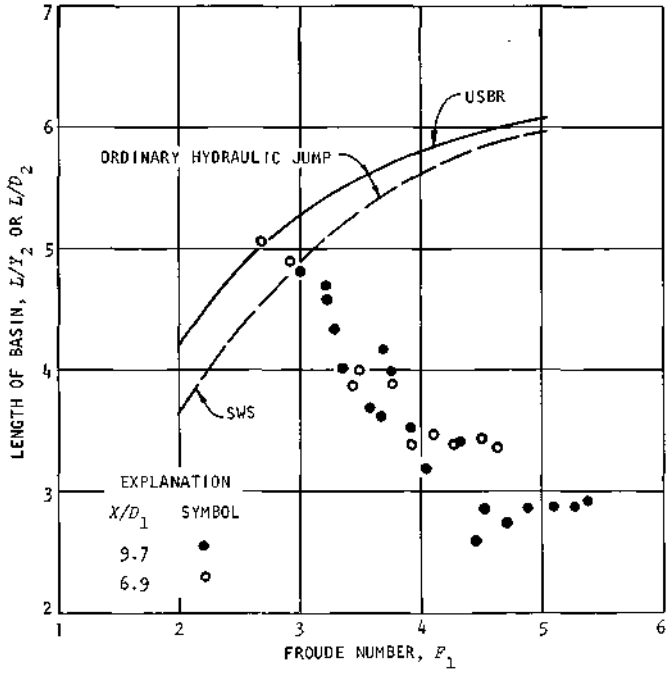

Figure 30. Length ratio for basin K

The arrangement of the baffles for basin K was altered to study the effects of baffle orientation on the general performance of the basin. All baffle blocks were rotated by exactly 180 degrees, keeping the relative positions the same as those given in figure 14d. The rotation of the baffles was done for the two spacings (X/D_1 = 6.9 and 9.7) between the baffles and the end sill. Test data with this modification showed no significant change in the performance of the basin compared with that of its original geometry.

Figures 31 and 32 show the typical flow conditions of basin K for X/D_1 of 9.7 and 6.9, respectively. Table 6 gives the data collected with both arrangements of basin K.

Basin L. Basin L is shown in figures 15a and 15b. It has already been noted that basins E, G, and H showed some promising results in comparison with other basins tested. A few other arrangements similar to these were then tried. After some trial-and-error testing, the arrangement shown in figure 15a as basin L was found to perform well in the range of flow conditions under consideration.

Except for minor variations, the arrangement shown is very similar to basin H. The baffles nearest the side walls in basin L are smaller than those in basin H. The height of the end sill is 0.06 foot, the same as that of basin K. The distance between the baffles and the end sill was shorter

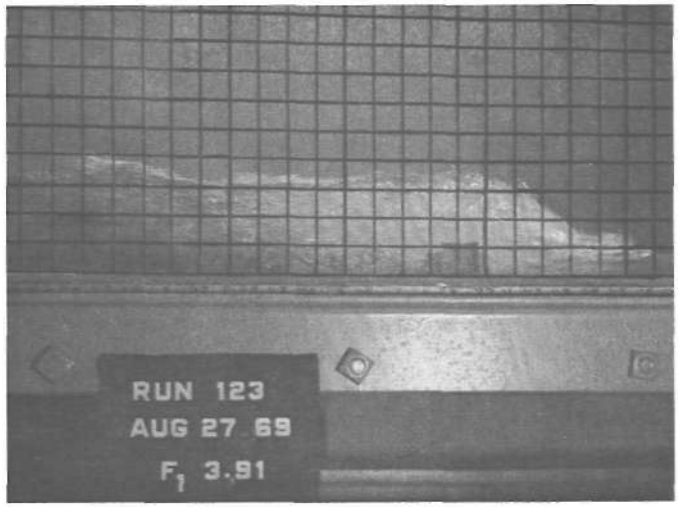

Figure 31. Flow conditions in basin K with longer distance between baffles and end sill

than for the other basins, but the oblique orientation of the baffles was maintained.

The main characteristics of basin L were: h_1/D_1 = 1.85; h_2/D_1 = 0.82; X/D_1 = 8.2; distance between the side wall and the nearest baffle was $1.5D_1$; the base width of the end sill was equal to twice the height of the end sill; the length of the baffles parallel to the direction of flow was $2.33D_1$; the width of the baffles was $1.23D_1$; the height of the baffle blocks was 2.25 times the height of the end sill; the side slope of the baffles in plan view was 1:3.78; and the clear space between the baffles either at the upstream or at the downstream section was $3.01D_1$. The total projected width of the baffles normal to the direction of flow was 37 percent of the total width of the flume. Figure 15b shows in detail the dimensions of the basin expressed in terms of upstream depth D_1.

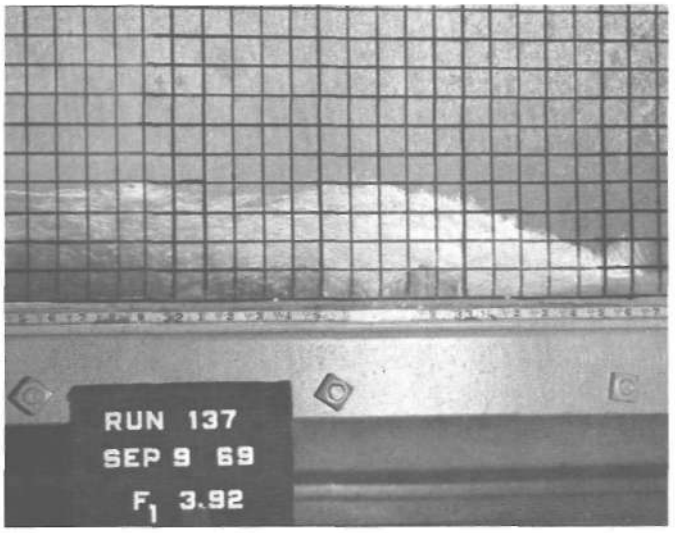

Figure 32. Flow conditions in basin K with shorter distance between baffles and end sill

During the investigation it was observed that the relative height and the spacing of the end sill with respect to the baffles were critical in the formation and propagation of the waves in the downstream portion of the channel. With increase in the height and spacing of the end sill, the generation of the waves was accelerated, and conversely, as the height and spacing were reduced to some extent, the wave activity was somewhat reduced. Pillai and Unny[7] observed similar effects due to the reduction of height and spacing between the end sill and baffle blocks.

The arrangement of basin L produced less disturbance near the centerline of the basin than did basins D through K. Visual observation also showed that the oblique orientation of the baffles had the desired effect, namely, forcing the high velocity jets to intermix thoroughly giving the appear-

Table 6. Test Data for Forced Hydraulic Jump, Basin K

Q (cfs)	D_1 (ft)	V_1 (fps)	F_1	E_1 (ft)	Y_2 (ft)	E_2 (ft)	$(E_L/E_1) \times 100$	Y_2/D_1	L (ft)	L/Y_2
				$h_1/D_1 = 1.71$, $h_2/D_1 = 1.14$, $X/D_1 = 10.0$						
0.61	0.069	4.42	2.96							
0.72	0.070	4.86	3.22	0.435	0.300	0.321	26.2	4.28	1.40	4.66
0.80	0.071	5.60	3.70	0.556	0.310	0.336	39.6	4.37	1.30	4.18
0.82	0.072	5.70	3.75	0.573	0.322	0.347	39.7	4.47	1.25	3.98
0.84	0.071	5.91	3.91	0.611						
				$h_1/D_1 = 1.66$, $h_2/D_1 = 0.833$, $X/D_1 = 9.7$						
0.67	0.073	4.60	3.00	0.399	0.260	0.286	28.3	3.56	1.25	4.80
0.71	0.072	4.93	3.23	0.448	0.208	0 309	31.0	3.96	1.30	4.56
0.73	0.073	5.00	3.26	0.460	0.305	0.327	29.0	4.16	1.32	4.33
0.75	0.073	5.14	3.35	0.481	0.317	0.334	30.5	4.27	1.25	4.00
0.78	0.072	5.41	3.56	0.527	0.327	0.349	33.8	4.54	1.20	3.67
0.80	0.072	5.57	3.66	0.553	0.335	0.357	35.4	4.65	1.21	3.60
0.85	0.072	5.96	3.91	0.622	0.356	0.378	39.2	4.95	1.25	3.52
0.88	0.072	6.11	4.01	0.651	0.376	0.397	39.1	5.21	1.20	3.19
0.95	0.072	6.60	4.33	0.745	0.400	0.422	43.3	5.56	1.35	3.38
0.98	0.072	6.81	4.46	0.792	0.407	0.429	45.8	5.67	1.05	2.58
0.99	0.072	6.87	4.51	0.803	0.420	0.442	45.0	5.84	1.20	2.86
1.05	0.073	7.19	4.71	0.873	0.438	0.461	47.2	6.01	1.20	2.74
1.07	0.072	7.42	4.87	0.923	0.454	0.476	48.5	6.30	1.30	2.86
1.12	0.072	7.77	5.10	1.000	0.471	0.493	50.7	6.55	1.35	2.86
1.16	0.072	8.05	5.29	1.073	0.486	0.508	52.6	6.75	1.40	2.86
1.18	0.072	8.20	5.37	1.092	0.498	0.520	52.5	6.91	1.45	2.91
				$h_1/D_1 = 1.64$, $h_2/D_1 = 0.82$, $X/D_1 = 6.9$						
0.77	0.073	5.28	3.44	0.504	0.298	0.324	35.7	4.07	1.15	3.86
0.82	0.073	5.61	3.49	0.560	0.339	0.362	35.4	4.65	1.35	3.98
0.84	0.073	5.75	3.75	0.584	0.352	0.374	35.9	4.81	1.37	3.89
0.88	0.073	6.01	3.92	0.633	0.370	0.392	38.1	5.07	1.25	3.38
0.92	0.073	6.30	4.10	0.687	0.390	0.412	40.1	5.34	1.35	3.46
0.96	0.073	6.57	4.27	0.743	0.404	0.426	42.7	5.54	1.37	3.39
1.01	0.073	6.91	4.50	0.814	0.433	0.454	44.3	5.92	1.49	3.44
1.04	0.073	7.13	4.64	0.858	0.442	0.463	46.1	6.06	1.50	3.39
0.63	0.075	4.17	2.68	0.345	0.122					
0.63	0.075	4.17	2.68	0.345	0.242	0.268	22.3	3.23	1.22	5.05
0.67	0.074	4.53	2.93	0.391	0.260	0.286	26.8	3.51	1.30	4.88

ance of a uniform mixture of entrained air and water. Portions of the high velocity jets from each side of the centerline were forced to infringe on each other as a result of this arrangement.

The space between the side wall and the nearest baffle block was determined on the basis of disturbances in the downstream channel. Disturbances with the side wall were reduced when the side of the baffle block adjacent to the wall was made parallel to the wall. The front width of the baffles nearest the. side walls in basin L was smaller than that for similar basins. After testing several widths of baffle blocks, this smaller width of the baffle was found to generate a minimum amount of waves with the side wall.

To investigate the nature of the water surface profiles for different Froude numbers for basin L without any tail-water adjustment, basin L was tested with the following arrangements: end sill only, baffle blocks only, and end sill and baffle blocks. Then tests were made with end sill and baffle blocks but with adjustments in the tail-water depth. The profiles of the water surface for the end sill only and baffle blocks only are the same as those shown in figures 11 and 12.

Some typical water surface profiles with end sill and baffle blocks and no tail-water adjustment for various Froude numbers are given in figure 33. With an F_1 equal to 2.69, figure 33a, the flow in the downstream reach remained supercritical and F_2 was equal to 1.5. However, at this low Froude number, some waves were generated near the appurtenances and continued downstream. The location of the jump remained steady with little variation in the water surface profiles. With the increase in the F_1 value to 2.93, figure 33b, the water surface profiles fluctuated between two distinct profiles with supercritical flow in the downstream reach. For only a small increase in F_1 from 2.93 to 3.07, figure 33c, the characteristics of the water surface profiles changed, developing two different profiles, one with the side wall and another near the baffle blocks. The profile near the baffle blocks resembled a boil across the width of the flume. The profiles remained essentially steady with little fluctuation. Although the depth of water increased greatly in the boil, the water surface profile close to the wall remained considerably lower than the boil height. This is particularly important when there is not enough tail-water depth to stabilize the jump in the basin. With further increase in the F_1 value to 3.57, figure 33d, the general nature of the water surface profiles remained the same as for F_1 = 3.07, except that an air pocket developed above the top of the baffles and high velocity water flowed downstream on all sides of this air pocket. The nature of the profiles remained the same for higher Froude numbers up to 4.5 as long as the relative height of the baffles with upstream depth remained the same.

The above discussion indicates that for the full development of a hydraulic jump, the tail-water depth must be adjusted in the laboratory flume. For practical field application, the stilling basin would be depressed, increasing the depth of water to stabilize the jump in the basin. Thus, all

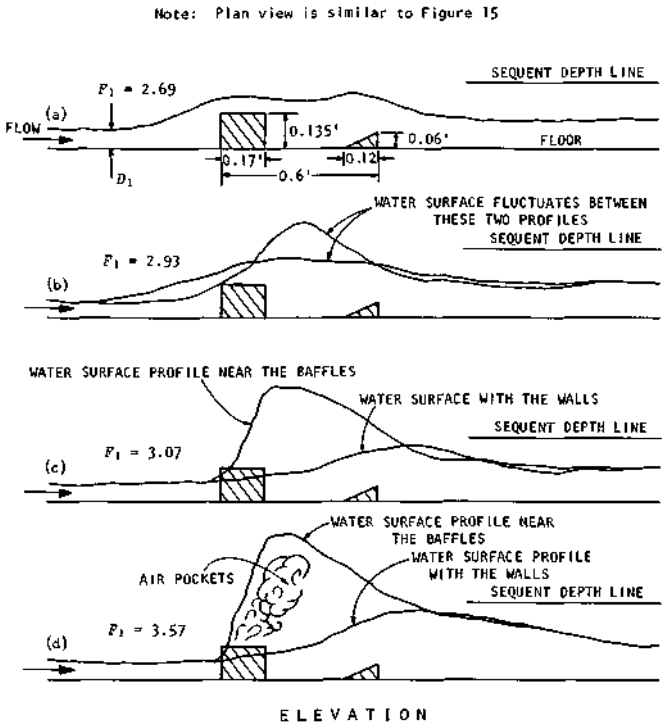

Figure 33. Water surface profiles for basin L without tail-water adjustment

subsequent tests were conducted by adjusting the tail-water depth in addition to using the appurtenances already mentioned for basin L. The tail-water depth was increased or decreased with each run to observe the nature and the stability of the jump. When the jump appeared to be well established with only minor fluctuation, the pertinent data were collected.

From an analysis of the data collected from basin L, it was observed that the toe of the jump should be placed at a distance of approximately $3(D_2 - D_1)$ from the upstream side of the baffle blocks. If the distance between the toe of the jump and the baffles is increased, the full effectiveness of the baffles cannot be attained because of the presence of a higher water level upstream of the baffle blocks. If the distance between the baffles and the toe of the jump is decreased, the jump becomes unstable with an associated forward and backward movement of the jump, and this results in considerable wave generation in the downstream reach of the channel.

Discussion of Basin L Test Results

Tail-Water Depth. The relationship between the depth ratio Y_2/D_1 and F_1 is shown in figure 34 for basin L. A similar relationship for an ordinary hydraulic jump in a rectangular basin is also given for reference. An average line drawn through all the data collected for basin L falls below the line for an ordinary hydraulic jump. The average line for basin L indicates that the tail-water depth required for the stability of the jump is generally less than the sequent depth for the same Froude number. The depth ratio is about

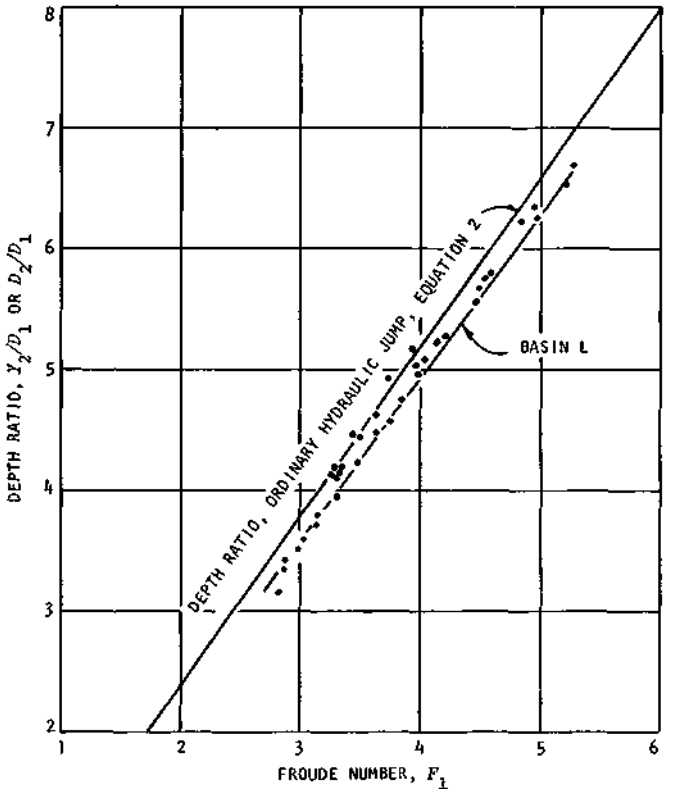

Figure 34. Relationship between depth ratio and Froude number for basin L

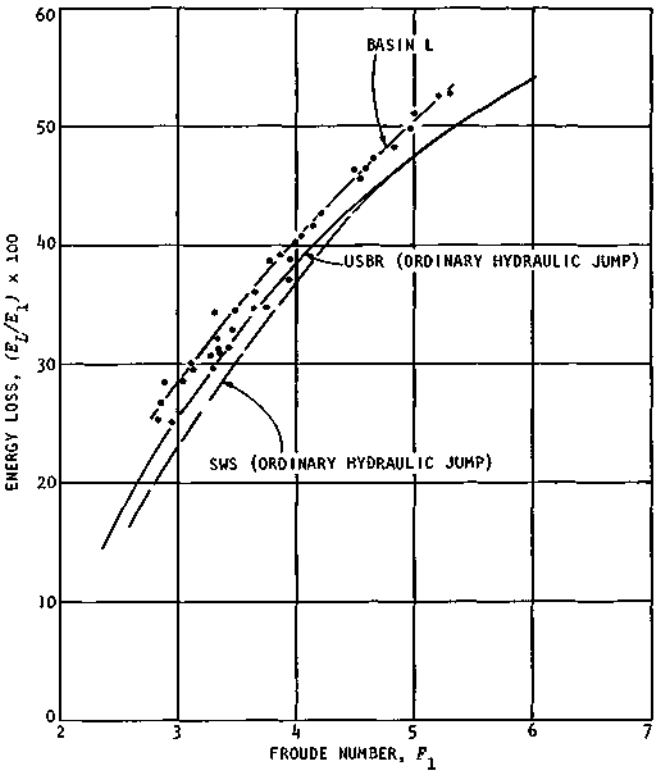

Figure 35. Energy loss in basin L

5 percent smaller for basin L, in comparison with the ordinary hydraulic jump. Knowing this variation will enable the designer to predict the required tail-water depth when the sequent depth is known.

Although the tail-water depth required is about 5 percent less than the sequent depth, increasing the tail-water depth to the sequent depth will, in fact, increase the stability of the jump. Also, increasing the depth reduces the wave action downstream from the stilling basin. USBR[1] recommended a tail-water depth Y_2 of 5 to 10 percent greater than the sequent depth D_2 for F_1 range of 2.5 to 4.5. From a model study for McNary Dam with F_1 = 3.3, Berryhill[22] reported that the apron elevation was set so that the maximum tail-water depth was equal to 90 percent of the sequent depth. The same author reported that from prototype observations the jump performed very well with this recommended tail-water depth and for even smaller tail-water depths. In the SAF stilling basins[2] the tail-water depth was made equal to 85 percent of the sequent depth. However, it should be noted that all of these stilling basins with a horizontal apron containing baffle blocks and end sill were constructed at the end of a chute equipped with chute blocks. The flow dynamics are therefore different from those occurring below a sluice gate. This may explain why the tail-water depth required below a sluice gate is higher than that required in the stilling basins described above. However, in both cases, a tail-water depth equal to the sequent depth will substantially increase the stability of the jump.

Energy Loss. The relationship between the nondimensional energy loss expressed as E_L/E_1 and F_1 is shown in figure 35 for basin L. An average curve has been drawn for the data, and the curves from the USBR[1] and SWS studies for the ordinary jumps are shown. Comparison of the curves shows that the energy loss E_L/E_1 for basin L in increased by approximately 3 percent compared with the USBR curve and by about 3 to 4.5 percent compared with the SWS data. This increase in energy loss indicates a smaller tail-water depth requirement compared with the ordinary jump and the effectiveness of the appurtenances in reducing the depth of flow for constant discharge. Thus, the present arrangement of the basin contributed to increasing the energy loss E_L/E_1 by approximately 3 to 4 percent. This increase in energy loss compares favorably with the data reported by Peterka[1] and Rajaratnam[8] under similar flow conditions.

The energy loss can also be expressed in a slightly different form. With a constant discharge, the specific energy content of the flow is minimum at the critical stage of flow, i.e., this is the minimum energy at which the flow can exist (figure 7). Therefore, the difference between the energy content at the supercritical depth of flow and the energy content at the critical depth of flow is the maximum available amount of energy that can be dissipated. Since the maximum energy available for dissipation is $E_1 - E_c$, the percentage of energy lost, P_L, can be expressed as

$$P_L = [E_L/(E_1 - E_C)]100 \qquad (14)$$

Although $E_1 - E_c$ is available for possible dissipation, this is undesirable because the resulting critical velocity

would be large and would probably result in excessive erosion and scour of the channel bed and banks. The hydraulic jump type stilling basin insures the development of a subcritical flow stage in the downstream channel, and serves to protect the channel.

The head loss of the jump as expressed by equation 14 has been computed for basin L and the graphical relationship between P_L and F_1 is shown in figure 36. The plot indicates that there is some scatter in the experimental data from the average line for a Froude number between 2.8 and 3.7. Fluctuations in the downstream water surface profiles were observed in this range of the Froude number with some associated wave generation. The depth of water was computed from an average of three measurements and the mean value was taken to be the average depth. The wave generation and the fluctuating nature of the flow may explain the scatter in the plotted points in figure 36. With an increase in the value of F_1, the jump stabilizes with considerable reduction in the wave activity, and the plotted points fall very close to the average line.

In terms of the energy available for dissipation, figure 36 shows that the energy loss $[E_L/(E_1 - E_c)]$ varies from about 62 to 73 percent as F_1 varies from 2.8 to 4.5. The percentage of energy loss shown in figure 36 is larger than that in figure 35 because of the different base utilized in computing the energy losses plotted in these figures.

The 3 to 4.5 percent increase in energy loss shown in figure 35 may appear to be small, which might indicate that the hydraulic jump type basin is not an efficient energy dissipating device. But it must be remembered that E_c is not available for dissipation (figure 7) and hence when the comparison of energy loss is based on P_L (figure 36) it is clear that the jump is very efficient as far as energy loss is concerned.

Length of the Basin. One of the most important parameters in the design of a stilling basin is the length of the basin required for the stability of the jump. Although the jump can be stabilized from a hydraulic point of view with proper adjustment in the tail-water depth, the length of the basin thus required is in most instances not desirable from economical considerations. Any reduction in the length of the basin without sacrificing a stable jump would result in a considerable cost saving in the construction of the stilling basin. Thus the main benefit derived from the appurtenances in the stilling basin is the reduction in the length of the basin, although they also help to stabilize the jump.

In this study the length of the jump was considered to be the distance between the toe of the jump and the end sill. However, in some instances visual observation indicated that the jump stablized some distance upstream of the end sill. With a change in the Froude number, the length of the jump also varied. In this study the distance between the end sill and baffles was arranged so that the jump was always stable and the length of the basin was adequate to cover the full range of the Froude numbers 2.5 to 4.5.

The graphical relationship between the nondimensional ratio of L/D_2 with F_1 is shown in figure 37 for basin L. The sequent depth D_2 corresponding to F_1 has been computed from equation 2 for a hydraulic jump on a horizontal floor in a rectangular basin.

The stability of the jump is controlled in part by the tail-water depth. Thus it is reasonable and appropriate to express the required length of the basin as a function of the tail-water depth. Since the required tail-water depth for design purposes is initially an undetermined quantity, the length of the basin is generally expressed as a function of the sequent depth D_2, which can be determined easily. This type of relationship permits one to transpose the laboratory results to practical design applications. Most of the research[1,2] on the length of the stilling basin has been related to the sequent depth rather than the upstream depth.

The data plotted in figure 37 show that as the value of

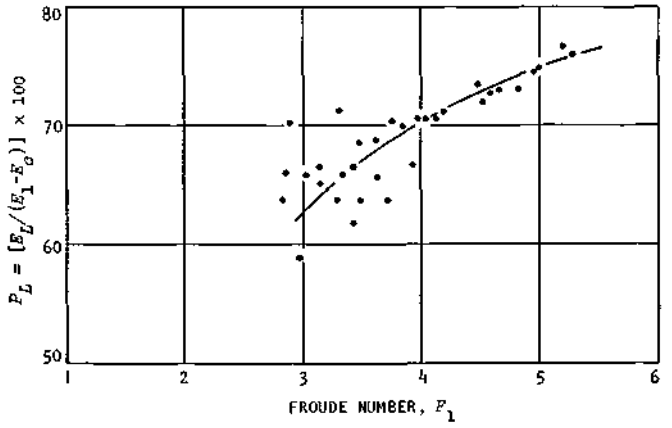

Figure 36. Energy loss in basin L based on maximum energy available for dissipation

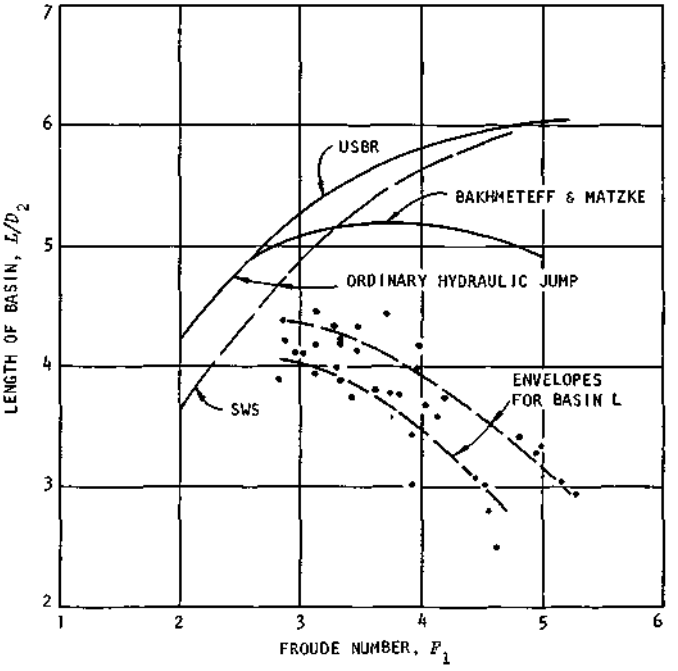

Figure 37. Length ratio for basin L

the Froude number increases (F_1 greater than 2.8), the length ratio L/D_2 decreases. The maximum value of the length ratio is at a Froude number of approximately 2.8, and this value appears to approach the length ratio for the ordinary hydraulic jump. At lower Froude numbers, the jump is transitional with intermittent formation and release of eddies making it very difficult to stabilize the jump within a shorter basin.

Increasing the tail-water depth above the sequent depth may submerge the jump altogether with a resulting high velocity jet near the floor of the basin. As soon as the tail-water depth is increased to a value close to the sequent depth, the jump can be stabilized with the addition of appurtenances. However, the relative length of the basin is larger for smaller F_1 than that necessary for higher Froude numbers within the range being considered. For the forced hydraulic jump Peterka[1] recommended utilizing the full length of the basin required for an ordinary hydraulic jump for the F_1 range of 2.5 to 4.5. But, figure 37 shows for basin L that only near an F_1 value of 2.8 is the length of the basin required very close to that required for the ordinary hydraulic jump. For higher Froude numbers the length ratio is much smaller than that required for the ordinary hydraulic jump.

The length ratio for basin L in figure 37 varies from about 4.4 for F_1 equal to 2.8 to about 3.5 for F_1 equal to 4.5. These values compare favorably with model studies conducted for outlet works of spillways.[22] As an example, the length of the basin, from the point of inflection of the spillway bucket curve to the lower end of the end sill, equal to $3D_2$ was sufficient for McNary Dam as reported by Berryhill.[22] The value of the upstream Froude number was 3.3 and two rows of staggered baffles and an end sill were utilized. The ASCE Task Force on Energy Dissipators for spillways and outlet works pointed out[23] that baffle piers and chute blocks used together with a simple end sill to prevent erosion can reduce the required length of the basin by approximately one-third compared with the length required for an ordinary hydraulic jump.

Compared with the USBR curve, the reduction in the length ratio of basin L (upper curve in figure 37) varied from about 15 percent for F_1 equal to 2.8 to about 41 percent for F_1 equal to 4.5. The same comparison for basin L with the data from the SWS study indicates a length ratio reduction varying from 7 percent at an F_1 of 2.8 to 40 percent for an F_1 of 4.5. Thus it is very reasonable and appropriate to indicate that a considerable saving can be attained in the construction of a basin by the reduction in the length required for the stability of the jump as obtained with basin L.

One of the main objectives and possibly the major aim in stilling basin design is to reduce the required length of the basin without sacrificing a well-developed hydraulic jump within the range of Froude numbers under consideration. Since it is very costly to construct a basin longer than necessary, the reduction in the length requirement is a major bonus for a fully stable hydraulic jump. Blaisdell[2] also pointed out that the reduction of the length of the basin is the major role of the baffles rather than excess energy dissipation. From this point of view, basin L seems to perform well within the range of Froude numbers under consideration.

Figures 38, 39, and 40 show the flow conditions in basin L. The data collected for basin L are given in table 7.

Waves and Cavitation in the Stilling Basin

Although attempts were made to eliminate all waves in the downstream channel, unfortunately these efforts were not successful in the basins tested. Some waves were present in all of the basins, but comparatively smaller waves were found to develop in basin L. The waves developed in the flume propagated for some distance downstream and finally disintegrated to small ripples. The propagation of the waves was assisted to some extent by the smooth wall of the flume. This would be completely different in the practical case where the rough bed and banks would offer more resistance to the flow and assist in damping the waves. Spill that might

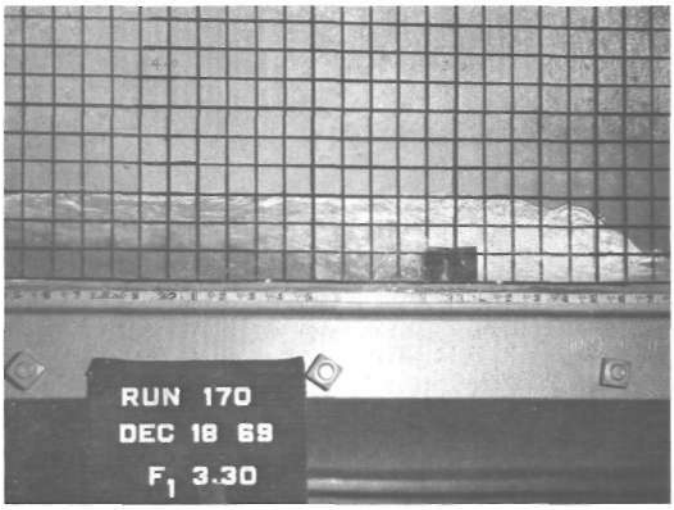

Figure 38. Flow conditions in basin L, Froude number of 3.30

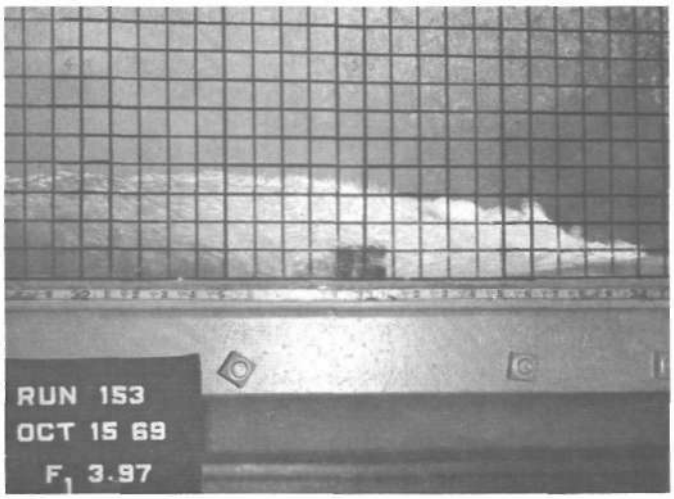

Figure 39. Flow conditions in basin L, Froude number of 3.97

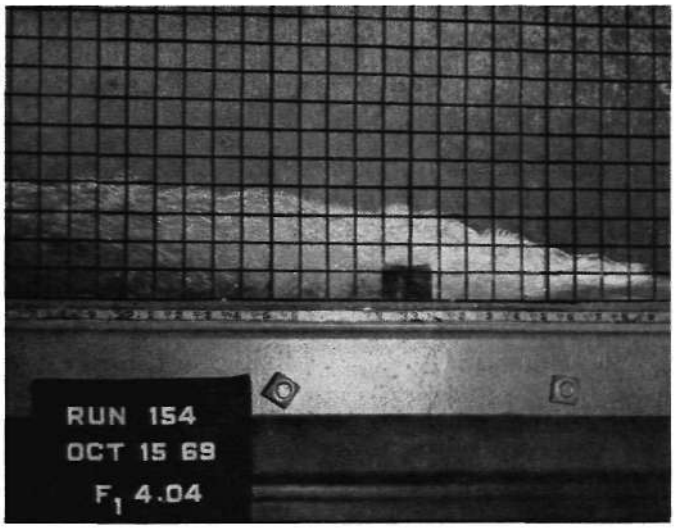

Figure 40. Flow conditions in basin L, Froude number of 4.04

occur because of waves can be prevented by the proper design of freeboard.

Data on cavitation of the baffles were not collected. The cavitation damage may not be as serious for F_1 in the range from 2.5 to 4.5 as it would be for higher Froude numbers.[16] The fluctuating nature of the water surface profiles associated with the flow at the low Froude number range makes it extremely difficult to collect any reliable data on pressure fluctuations on the baffle blocks. However, the theoretical relationships described by equations 8 and 9 can be utilized to predict the approximate magnitude of the turbulent pressure fluctuations in the stilling basin. This will be particularly helpful for the structural design of the chute, the stilling basin floor, and the baffle blocks. The only unknown quantity in equation 8 is the magnitude of relative turbulence, Σ / V. This value can be estimated[19,20] and related computations can be made to predict the magnitude of the turbulent pressure fluctuations.

Table 7. Test Data for Forced Hydraulic Jump, Basin L

Q (cfs)	D_1 (ft)	V_1 (fps)	F_1	E_1 (ft)	E_r (ft)	Y_2 (ft)	D_2 (ft)	E_2 (ft)	$(E_1/E_2) \times 100$	$(E_L/E_1 - E_r) \times 100$	Y_2/D_1	L (ft)	L/D_2
0.64	0.074	4.33	2.80	0.364	0.221								
0.68	0.074	4.60	2.97	0.400	0.230	0.259	0.269	0.300	25.0	58.9	3.50	1.10	4.09
0.70	0.073	4.79	3.12	0.428	0.234	0.273	0.292	0.299	30.1	66.5	3.74	1.30	4.45
0.74	0.073	5.11	3.33	0.478	0.244	0.300	0.311	0.324	32.2	65.9	4.11	1.30	4.18
0.77	0.073	5.27	3.42	0.504	0.249	0.325	0.321	0.347	31.3	61.6	4.45	1.20	3.74
0.82	0.074	5.59	3.61	0.558	0.261	0.330	0.346	0.354	36.6	68.7	4.46		
0.84	0.073	5.75	3.75	0.585	0.265	0.334	0.352	0.359	38.7	70.5	4.57	1.32	3.75
0.86	0.073	5.89	3.84	0.609	0.269	0.347	0.365	0.371	39.2	70.0	4.75	1.37	3.75
0.89	0.073	6.10	3.97	0.648	0.275	0.363	0.378	0.386	40.4	70.2	4.97	1.50	3.96
0.91	0.073	6.20	4.04	0.667	0.278	0.370	0.384	0.393	40.7	70.2	5.07	1.40	3.65
0.92	0.073	6.34	4.13	0.693	0.282	0.382	0.394	0.405	41.6	70.2	5.24	1.40	3.55
0.94	0.073	6.44	4.20	0.714	0.285	0.386	0.401	0.409	42.7	71.1	5.30	1.50	3.73
1.01	0.073	6.92	4.51	0.815	0.298	0.421	0.434	0.443	45.6	72.0	5.76	1.30	3.00
1.00	0.073	6.84	4.46	0.798	0.296	0.405	0.428	0.429	46.2	73.4	5.55	1.30	3.04
1.02	0.073	7.00	4.56	0.832	0.301	0.424	0.438	0.446	46.4	72.6	5.81	1.22	2.78
1.04	0.073	7.12	4.62	0.858	0.308	0.429	0.445	0.452	47.3	73.7	5.86	1.11	2.47
1.08	0.073	7.40	4.81	0.922	0.312	0.455	0.464	0.477	48.2	73.0	6.23	1.58	3.40
1.11	0.073	7.60	4.95	0.967	0.318	0.462	0.478	0.484	49.8	74.4	6.34	1.56	3.26
1.14	0.074	7.71	4.99	0.995	0.324	0.462	0.457	0.486	51.1	74.7	6.25	1.54	3.34
1.16	0.073	7.97	5.19	1.058	0.329	0.476	0.503	0.499	52.7	76.5	6.52	1.51	3.00
1.18	0.073	8.07	5.26	1.083	0.331	0.490	0.512	0.512	52.7	75.9	6.70	1.50	2.93
0.67	0.076	4.41	2.82	0.376	0.227	0.254	0.271	0.281	25.3	63.8	3.16	1.05	3.86
0.67	0.075	4.46	2.87	0.382	0.227	0.257	0.274	0.283	28.5	70.3	3.42	1.15	4.20
0.68	0.073	4.62	3.01	0.404	0.228	0.262	0.281	0.288	28.7	65.9	3.59	1.15	4.09
0.70	0.073	4.80	3.12	0.429	0.234	0.277	0.292	0.302	29.6	65.0	3.79	1.15	3.94
0.74	0.073	5.07	3.30	0.470	0.243	0.288	0.310	0.308	34.5	71.3	3.95	1.23	3.97
0.77	0.073	5.31	3.46	0.510	0.253	0.310	0.327	0.334	34.5	68.5	4.24	1.35	4.12
0.81	0.073	5.55	3.62	0.550	0.258	0.337	0.343	0.359	34.7	65.5	4.62	1.30	3.79
0.75	0.073	5.14	3.34	0.482	0.244	0.308	0.311	0.331	31.4	63.5	4.21	1.20	3.86
0.64	0.073	4.38	2.85	0.370	0.220	0.244	0.263	0.271	26.7	66.0	3.34	1.15	4.36
0.72	0.072	5.00	3.28	0.458	0.238	0.295	0.302	0.318	30.6	63.6	4.10	1.30	4.31
0.75	0.073	5.00	3.28	0.458	0.238	0.301	0.302	0.323	29.5	63.6	4.18	1.30	4.31
0.75	0.073	5.14	3.34	0.482	0.244	0.309	0.308	0.332	31.1	63.1	4.23	1.30	4.22
0.78	0.073	5.34	3.48	0.514	0.251	0.325	0.323	0.347	32.5	63.5	4.44	1.40	4.32
0.84	0.073	5.75	3.74	0.584	0.264	0.359	0.349	0.380	34.9	63.7	4.92	1.55	4.44
0.86	0.072	5.96	3.93	0.623	0.268	0.364	0.368	0.386	38.1	66.8	5.06	1.25	3.40
0.88	0.073	6.03	3.92	0.634	0.273	0.378	0.367	0.399	37.1	65.0	5.18	1.10	3.00

SUMMARY

Design of hydraulic jump type stilling basins is a combination of practical experience, theoretical analysis, and model studies or laboratory investigations. No two stilling basins perform exactly the same in all respects; however, a generalized design criteria can be attained for stilling basins subjected to similar flow conditions and performing under similar circumstances.

Laboratory tests were conducted to obtain improved design criteria for stilling basins in the Froude number range of 2.5 to 4.5. Tests were made in a 2-foot-wide glass walled tilting flume, in which the supercritical depth was established with a sluice gate and downstream depth could be controlled with a tailgate to simulate the tail-water depth.

Data were collected for both the ordinary hydraulic jump and the forced hydraulic jump for a rectangular basin on a horizontal floor. Appurtenances such as baffle blocks and end sills were used to force the jump to form at a particular location.

Graphical relationships were developed for both the ordinary hydraulic jump and the forced hydraulic jump in the Froude number range of 2.5 to 4.5. The three nondimensional variables — the depth ratio D_2/D_1, the energy loss ratio E_L/E_1, and the length ratio L/D_2 — were related independently with the Froude number F_1.

Relationships developed from data collected for the ordinary hydraulic jump showed good agreement with published data from other laboratories and with the theoretical relationship expressed by equation 2.

The sequent depth D_2, energy loss E_L, and length of the basin L for ordinary hydraulic jumps can easily be estimated from figures 8, 9, and 10 when the supercritical Froude number F_1 and flow depth D_1 are known.

The concerted action of tail water, baffle blocks, and end sill stabilizes the hydraulic jump on the apron, dissipates much of the energy of the high velocity flow that enters the stilling basin, and can force the jump to form at the entrance section of the basin. The hydraulic jump that is generated as a result of the cumulative efforts of different appurtenances and the tail-water depth is termed the forced hydraulic jump.

Experimental investigations on stilling basins equipped with various geometrical arrangements of appurtenances either in combination or individually were conducted, and those for basins D through L are described in detail. The performances of these forced hydraulic jump type basins were judged by comparison with corresponding data for the ordinary hydraulic jump.

Basin L (figure 15) was found to perform satisfactorily for the range of Froude number from 2.5 to 4.5. This basin can be successfully adopted for practical applications with considerable savings in the construction cost of the stilling basin without sacrificing a stable hydraulic jump.

The relationship between F_1 and depth ratio Y_2/D_1 for a forced hydraulic jump in basin L (figure 34) shows that the required depth ratio can be decreased by 5 percent from that required with an ordinary jump. However, to improve the stability of the jump and also to damp the waves in the downstream channel, it is recommended that the tail-water depth be made equal to the sequent depth for the range of Froude number from 2.5 to 4.5.

In comparison with the ordinary hydraulic jump, the energy loss E_L/E_1 with basin L can be increased by about 4.5 to 3 percent for a variation in F_1 from 2.8 to 4.5, respectively (figure 35). This energy loss with basin L may not seem to be a significant amount. However, the energy E_c associated with critical depth (figure 7) is not available for dissipation, and when the energy loss for basin L is expressed as a function of the available amount of energy $(E_1 - E_c)$, as given by equation 14, it varies from 62 to 73 percent as F_1 varies from 2.8 to 4.5 (figure 36). This indicates that hydraulic jump type stilling basins are in fact very efficient in dissipating the supercritical flow energy.

Reduction in the required length of the basin would account for substantial savings toward the total cost of a stilling basin. The length ratio L/D_2 in basin L is 7 to 40 percent less than that required for the ordinary hydraulic jump when F_1 varies from 2.8 to 4.5 (figure 37).

The relationships developed for basin L in figures 34, 35, and 37 can be utilized to predict the required downstream depth, amount of energy loss, and the length of the basin, respectively, from a knowledge of the total discharge, upstream width, and depth of water in the basin. Estimation of the upstream depth of water will depend on the flow geometry, head of water, discharge, and configuration of the spillway or other outlet works.

Analytical expressions (equations 8 and 9) have been developed to predict the turbulent pressure fluctuations associated with turbulent velocity fluctuations in a stilling basin. Knowledge of turbulent pressure fluctuations is important not only to design the chute face and chute blocks against uplift, but also to indicate the amount and the extent of cavitation damages that can be expected on the chute block faces. In equations 8 or 9 the relative intensity of turbulence σ/V is unknown and must be estimated from experimental results such as those given in figure 2.

Some wave action was found to be present in the downstream channel in all cases. The arrangement of appurtenances for basin L (figure 15) produced less disturbance than the other basin arrangements tested.

All the graphical relationships have been developed from data collected for an upstream Froude number variation of about 2.5 to 4.5. Although it was observed that basin L performs particularly well in the higher Froude numbers from about 3.5 to 4.5, the relationship may not be extrapolated for Froude numbers greater than 4.5.

REFERENCES

1 Peterka, A. J. 1963. *Hydraulic design of stilling basins and energy dissipators.* U.S. Bureau of Reclamation, Engineering Monograph 25, 222 p.

2 Blaisdell, F. W. 1948. *Development and hydraulic design St. Anthony Falls stilling basin.* Transactions American Society of Civil Engineers v. 113:483-520.

3 Harleman, D. R. F. 1955. *Effect of baffle piers on stilling basin performance.* Journal of Boston Society of Civil Engineers v. 42:84-99.

4 Forster, J. W., and R. A. Skrinde. 1950. *Control of the hydraulic jump by sills.* Transactions American Society of Civil Engineers v. 115:973-987.

5 Rand, W. 1957. *An approach to generalized design of stilling basins.* Transactions New York Academy of Science (series 2) v. 20:173-191.

6 Rand, W. 1965. *Flow over a vertical sill in an open channel.* Proceedings ASCE, Journal of the Hydraulics Division v. 91 (HY4): 97-121.

7 Pillai, N. N., and T. E. Unny. 1964. *Shapes for appurtenances in stilling basins.* Proceedings ASCE, Journal of the Hydraulics Division v. 90(HY3) : 1-21.

8 Rajaratnam, N. 1967. *Hydraulic jumps. In* Advances in Hydrosciences, by V. T. Chow (ed.), Academic Press, New York and London, v. 4:197-280.

9 Rouse, H. 1970. *Work-energy equation for the streamline.* Proceedings ASCE, Journal of the Hydraulics Division v. 96(HY5): 1179-1190.

10 Bakhmeteff, B. A., and A. E. Matzke. 1936. *The hydraulic jump in terms of dynamic similarity.* Transactions American Society of Civil Engineers v. 101: 630-647.

11 Rajaratnam, N., and K. Subramanya. 1968. *Profile of the hydraulic jump.* Proceedings ASCE, Journal of the Hydraulics Division v. 94(HY3): 663-673.

12 Basco, D. R. 1969. Discussion of Proceeding Paper 5931. Proceedings ASCE, Journal of the Hydraulics Division v. 95(HY1):549.

13 Tsubaki, T. 1950. *Theory of hydraulic jump.* Kyushu University, Fukuoka, Japan, Reports of Research Institute for Fluid Engineering v. 6(2) : 99-106.

14 Kindsvater, C. E. 1944. *The hydraulic jump in sloping channels.* Transactions American Society of Civil Engineers v. 109:1107-1154.

15 Rajaratnam, N. 1964. *The forced hydraulic jump.* Water Power v. 16:14-19, 61-65.

16 U.S. Bureau of Reclamation. 1963. *Research study on stilling basins energy dissipators and associated appurtenances: Section 12, Stilling basin chute block pressures.* Hydraulic Branch Report HYd-514, 13 p.

17 Bhowmik, N. G. 1970. Discussion of Proceeding Paper 6915. Proceedings ASCE, Journal of the Hydraulics Division v. 96(HY7) : 1641.

18 Bakhmeteff, B. A. 1962. *Advance computations of hydraulic forces* (Appendix B). *In* Review of Research on Channel Stabilization of the Mississippi River 1931-1962, by J. B. Tiffany, U.S. Army Corps of Engineers, Vicksburg, Mississippi, B1-B9.

19 Bhowmik, N. G. 1968. *The mechanics of flow and stability of alluvial channels formed in coarse materials.* Ph.D. dissertation, Colorado State University, Fort Collins, 207 p.

20 Bowers, C. E., and F. Y. Tsai. 1969. *Fluctuating pressures in spillway stilling basins.* Proceedings ASCE, Journal of the Hydraulics Division v. 95(HY6) :2071-2079.

21 Illinois State Water Survey. 1955. *Hydraulic laboratory research facilities of the Illinois State Water Survey.* Circular 48, 15 p.

22 Berryhill, R. H. 1957. *Stilling basin experiences of the Corps of Engineers.* Proceedings ASCE, Journal of the Hydraulics Division v. 83 (HY3) : 1264-1 to 1264-36.

23 Task Force on Energy Dissipators for Spillways and Outlet Works. 1964. *Progress report.* Proceedings ASCE, Journal of the Hydraulics Division v. 89(HY1): 121-149.

NOTATIONS

C = Turbulent convection in feet
C_d = Coefficient of drag, nondimensional
D = Total channel depth in feet
D_1 = Supercritical flow depth in feet
D_2 = Sequent depth in a rectangular basin in feet
E_1 = Specific energy of the supercritical flow in feet
E_2 = Specific energy of the subcritical flow in feet
E_c = Specific energy associated with critical depth of flow in feet
E_L = Energy loss in the hydraulic jump in feet
F_1 = Froude number associated with supercritical flow stage, nondimensional
F_2 = Froude number associated with subcritical flow stage, nondimensional
g = Acceleration due to gravity in feet per second per second
h = Height of the sill in feet
h_1 = Height of the baffle block in feet
h_2 = Height of the end sill in feet
h_c = Critical height of the sill in feet
H = Total head in feet
J = Dimensionless factor
K = Kinetic energy in feet
l = Head loss of the mean flow through either viscous dissipation or generation of turbulence in feet
L = Length of the basin in feet
L_{max} = Maximum length of the forced hydraulic jump which is equal to the corresponding length of the ordinary hydraulic jump in feet
L_{min} = Critical distance between the toe of the jump and the end sill when the jump is on the verge of moving out of the basin in feet
L_r = Length of the roller in feet
L_8 = Distance between the toe of the jump and the front of the sill in feet
M = Diffusion of energy due to mixing in feet
N = Sum of twice the relative intensity of turbulence and the square of the relative intensity of turbulence, nondimensional
p = Pressure" in pounds per square foot
p' = Pressure associated with the velocity $(V+v')$ in pounds per square foot
P = Piezometric head in feet
P_L = Percent energy loss in the hydraulic jump equal to $[E_L/(E_1-E_C)]100$
Q = Discharge in cubic feet per second
R = Reynolds number, nondimensional
S_t = Transfer of energy through shear in feet
v' = Instantaneous deviation of flow velocity from the mean in feet per second
V = Average flow velocity in feet per second
V_1 = Average supercritical flow velocity in feet per second
V_2 = Average subcritical flow velocity in feet per second
V_c = Critical flow velocity in a rectangular channel in feet per second
X = Longitudinal distance in the stilling basin in feet
y = Point depth of flow in feet
Y = Total depth of flow in feet
Y_c = Critical depth in a rectangular channel in feet
Y_2 = Tail-water depth in feet
r = Specific weight of water in pounds per cubic foot
Δp = Value of $(p—p')$ in pounds per square foot
e = Dissipation of energy in feet
$\sigma = \sqrt{\overline{v'^2}}$ = Standard deviation in feet per second